AN ABSTRACT OF THE THESIS OF

Yolanda H. Tennico for the degree of Master of Science in Chemistry presented on December 8, 2005
Title: Development of Materials and Devices for Separation of Polyamidoamine Dendrimers

Abstract approved:

Redacted for privacy

Vincent T. Remcho

Over the last decade, the use of highly branched macromolecules, called dendrimers, is emerging. Polyamidoamine (PAMAM) dendrimers, in particular, have attracted high interest due to their unique properties, such as well-defined size, shape, and solubility in water. Our group, as part of an interdisciplinary team, is currently working on developing a nanoextraction technology for high-yield dendrimer syntheses. Impurities may occur during the synthesis of these dendrimers, and therefore, to achieve higher purity products, chromatographic separations of dendrimers are an important part toward this goal. This thesis describes approaches toward this objective, focusing in two areas: at first, development of materials and devices that will enable separations of dendrimers in confines of capillary and chromatographic columns, and second, evaluation of the feasibility of transferring the separation techniques previously developed to the channels of microfluidic devices.

The results showed that PAMAM dendrimers of various generations were successfully analyzed using capillary zone electrophoresis (CZE), capillary

electrochromatography (CEC), and high-performance liquid chromatography (HPLC). Both CZE and HPLC have allowed for fast generational separations up to the fifth generation. Moreover, CZE can also assess the homogeneity and presence of side products in the synthesized dendrimers. RP-HPLC, on the other hand, allowed for separations of dendrimers with terminal amino and carboxyl groups.

PAMAM dendrimers can also be used as template molecules to prepare monolithic capillary columns for liquid chromatography and capillary electrochromatography. This method has provided two advantages: 1) dendrimers can be used as template molecules for controlling pore structures, 2) selective sorbents can be produced with surface sites that are complementary in chemical functionality to the dendrimer template molecule. These highly selective sorbents were able to provide separation of dendrimers from various generations, particularly of high generations, in the CEC mode.

As the first step toward the development of a nanoextraction technology for high yield dendrimer syntheses, the feasibility of extending the separation techniques developed on-column into channels of a microfluidic chip was examined. In this study, electrophoresis was employed to separate different generations of dendrimers in glass microfluidic chips using laser-induced fluorescence detection. The use of microfluidic system for dendrimer application offers great potential due to its rapid analysis times, small sample volume requirements, and the ability to integrate several steps of analyses in one chip.

Development of Materials and Devices for Separation of Polyamidomine Dendrimers

by
Yolanda H. Tennico

A THESIS

submitted to

Oregon State University

in partial fulfillment of
the requirements for the
degree of

Master of Science

Presented December 8, 2005
Commencement June 2006

Master of Science thesis of Yolanda H. Tennico presented on December 8, 2005.

APPROVED:

Redacted for privacy

Major Professor, representing Chemistry

Redacted for privacy

Chair of the Department of Chemistry

Redacted for privacy

Dean of the Graduate School

I understand that my thesis will become part of the permanent collection of Oregon State University libraries. My signature below authorizes release of my thesis to any reader upon request.

Redacted for privacy

Yolanda H. Tennico, Author

ACKNOWLEDGEMENTS

I would like to express my gratitude and appreciation to many people who have helped me in completing this thesis. Firstly, my deepest gratitude for my advisor, Dr. Vincent T. Remcho, without whom all of this could be possible. His help, guidance, suggestions, and encouragement have helped me tremendously in both research and writing of this thesis.

My sincere gratitude also for my committee members: Dr. Claudia Maier, Dr. Skip Rochefort, and Dr. Yun-Shik Lee. Thank you very much for your expertise, interest, and valuable advice.

Many thanks also to many collaborators: Dr. Chih-hung Chang (Dept. of Chemical Engineering), Dr. Brian Paul (Dept. of Industrial and Manufacturing Engineering), Shuhong Liu (Dept. of Chemical Engineering), Bindiya Abhinkar, Tom Tseng, and Eddie Blackwell (Dept. of Industrial and Manufacturing Engineering), Dr. Tom Plant, and Al Soeldner for giving me permission to use their facilities and assistance with my research work and data collection.

I would also like to thank the members of Remcho research group who have supported me in my research work: Dr. Angela Doneanu, Dr. Stacey Clark, Laura Lessard, Carlos Gonzalez, Jack Rundel, Myra Koesdjojo, Dana Hutanu, Bin Cao, and Corey Koch. Thank you for all your help and useful suggestions.

Lastly, I would like to thank my family and friends for their continuous supports and encouragements. Your great help in difficult times is highly appreciated. Thank you!

TABLE OF CONTENTS

TABLE OF CONTENTS (Continued)

TABLE OF CONTENTS (Continued)

LIST OF FIGURES

LIST OF FIGURES (Continued)

LIST OF FIGURES (Continued)

LIST OF TABLES

DEVELOPMENT OF MATERIALS AND DEVICES FOR SEPARATION OF POLYAMIDOAMINE DENDRIMERS

CHAPTER 1

INTRODUCTION TO DENDRIMERS: STRUCTURE, SYNTHESIS, PROPERTIES, AND APPLICATIONS

Linear macromolecules have traditionally been the most widely used polymeric materials. Recently, the use of highly branched macromolecules is emerging. One class of these is dendrimers from the Greek word 'dendron' meaning a tree. Dendrimers were first discovered by Tomalia et al [1] in the early 1980s and have attracted high interest during the last few years due to their unique properties, such as well-defined size, shape, and solubility in water. Thus, they have found numerous applications in chemical, physical, and biological processes. A large variety of dendrimers has been synthesized, e.g. polyamidoamines (PAMAM), polyethers, arborols, and polyamines, however PAMAM dendrimers, also known as Starburst dendrimers, are the most well-known and commonly used. This first chapter is intended to give an overview of dendrimers, in particular PAMAM dendrimers, in which their properties and applications will be discussed.

1.1.Synthesis of dendrimers

Dendrimers consist of three major structural components: 1) an initiator core, 2) repeating branched functional units connected to the core, and 3) end groups (fig. 1.1). Each repeating unit has a branching point onto which new repeating monomer units can be attached.

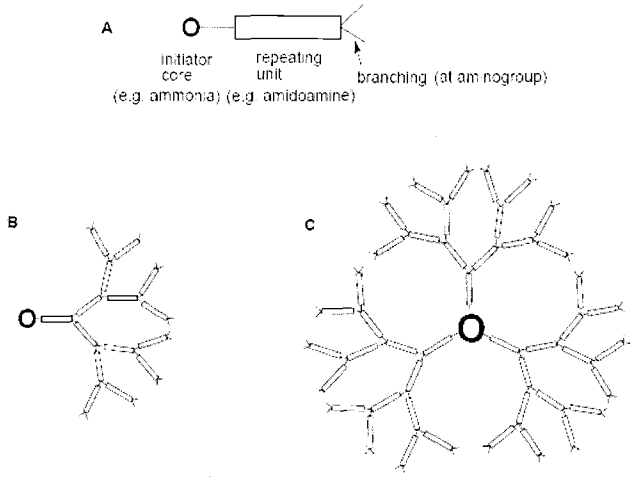

Fig 1.1. Architecture of dendritic macromolecules. (A) Structural elements, (B) dendrons, and (C) dendrimer [2].

The synthesis of dendrimers generally follows one of two major synthetic approaches: divergent or convergent [3]. In the divergent approach, dendrimers grow outward from the core molecule. The synthesis starts from the core and, step by step, layers (generations) are built around the core. The first generation dendrimers are created by reacting the core molecule with a functional monomer at the periphery. This process is then repeated to create the next generation by further reactions with monomers at the periphery (figure 1.2 A). In each generation, the

number of functional groups in the outermost layer increases exponentially with generation number.

In contrast to the divergent method (fig. 1.2 B), in the convergent approach, dendrimers grow inwards starting from the end group. They are constructed stepwise from the periphery to build the branched polymeric arms, called dendrons, to which a core molecule is finally attached. Therefore, the number of functional groups which have to react at any given step is reduced.

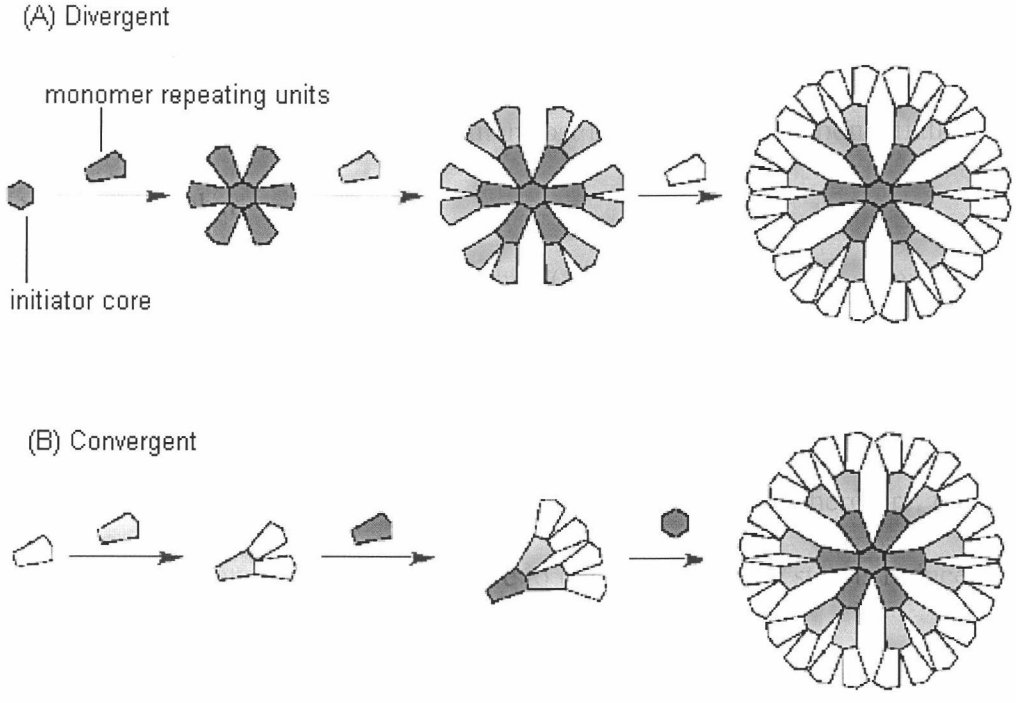

Fig. 1.2. (A) Construction of dendritic macromolecules by divergent growth, and (B) Convergent method [3]

There are some limitations with each of the two approaches. In the divergent approach, the conversion of functional groups must be 100% in order to obtain defect-free structures, however in reality, this is quite difficult to accomplish. Problems occurring from side reactions and incomplete reactions of the end groups that lead to structural defects often occur in the divergent method. A large excess of reagent is required to prevent these side reactions and force reactions to completion; however this presents difficulties in the purification of final product. This method, nevertheless, has proven successful to synthesize large amounts of dendrimers.

The convergent growth method minimizes the problems associated with the formation of side and incomplete reactions by precisely placing the functional group at the periphery of the macromolecule; however it generates steric problems in the attachment of dendrons to the core molecule when forming dendrimers of high generation.

PAMAM dendrimers can be synthesized by the divergent growth method through repetitive alkylation/amidation steps [4]. They are based on either an ammonia or ethylenediamine (EDA) core and possess amine groups at the periphery. Ammonia has three- and EDA has four-possible binding sites for amidoamine repeating units. The primary amino groups are on the surface of the molecule and two new branches may be attached to each of them.

When EDA is used as the core molecule, the synthesis consists of two consecutive steps: Michael addition of primary amine to methacrylate (MA), followed by the amidation of the multiester with EDA (fig. 1.3). At first, EDA

core molecule (generation G -1) is reacted with MA in the presence of methanol to create what is called a "half-generation" dendrimer (e.g. generation -0.5) since it possesses an anionic surface charge arising from carboxylate groups. Onto this molecule another EDA molecule is then added to create a "full-generation" dendrimer with four terminal amino groups (G 0), which have primary amine groups on the surface. At the periphery, the free amino group is further reacted with another MA monomers and EDA molecule. This two-step process is then repeated, with each reaction sequence resulting in a higher generation dendrimer. Hence, the number of terminal groups (table 1.1) is approximately doubled with the addition of each generation. The molecular masses increase exponentially with the addition of each generation (fig. 1.4)

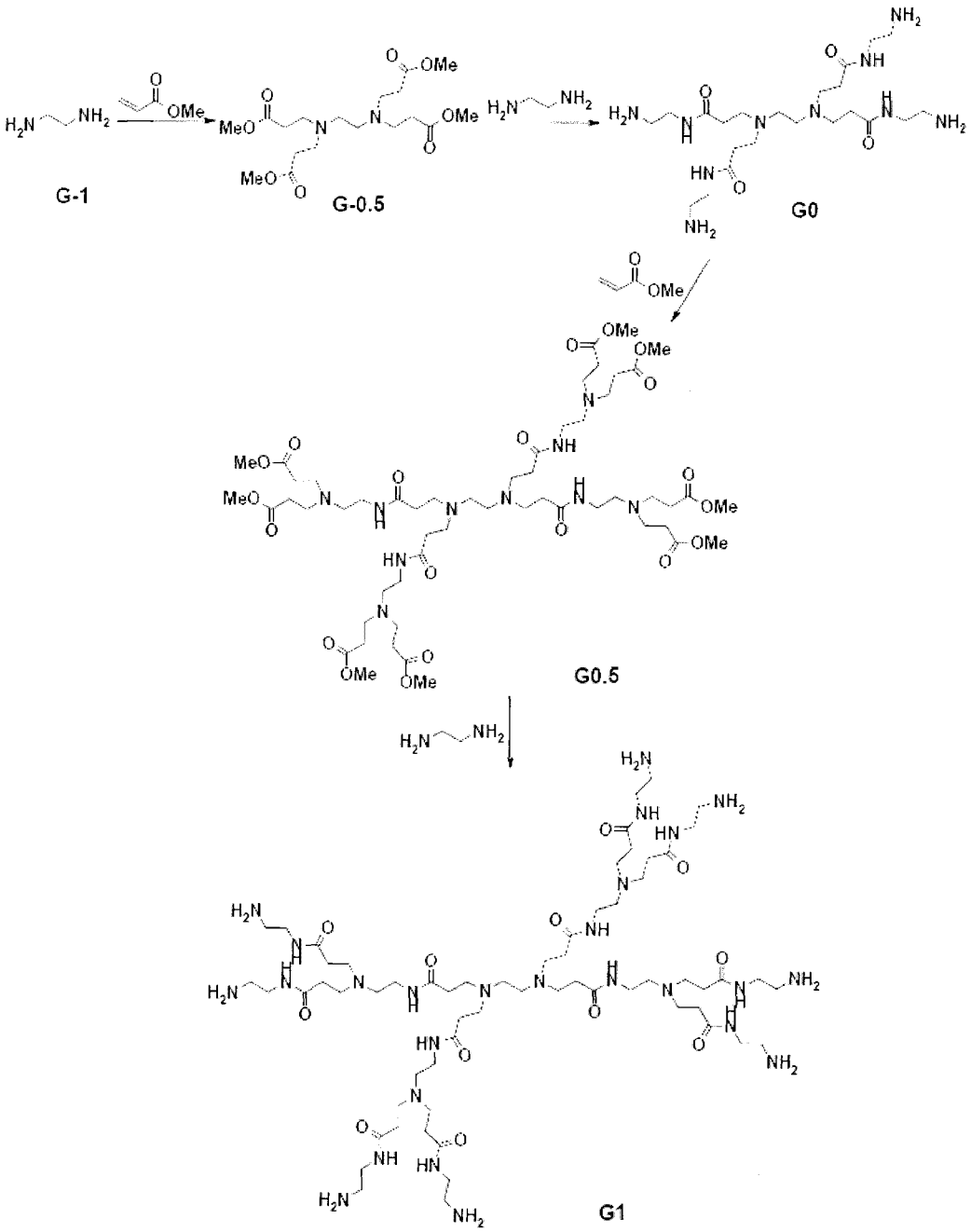

Figure 1.3: Synthesis of EDA-core PAMAM dendrimers [2]

Generation (EDA-core)	Molecular mass	Number of terminal groups
0	516	4
1	1428	8
2	3252	16
3	6900	32
4	14196	64
5	28788	128
6	57972	256
7	116340	512
8	233076	1024
9	466548	2048
10	933492	4096

Table 1.1. Properties of PAMAM dendrimers

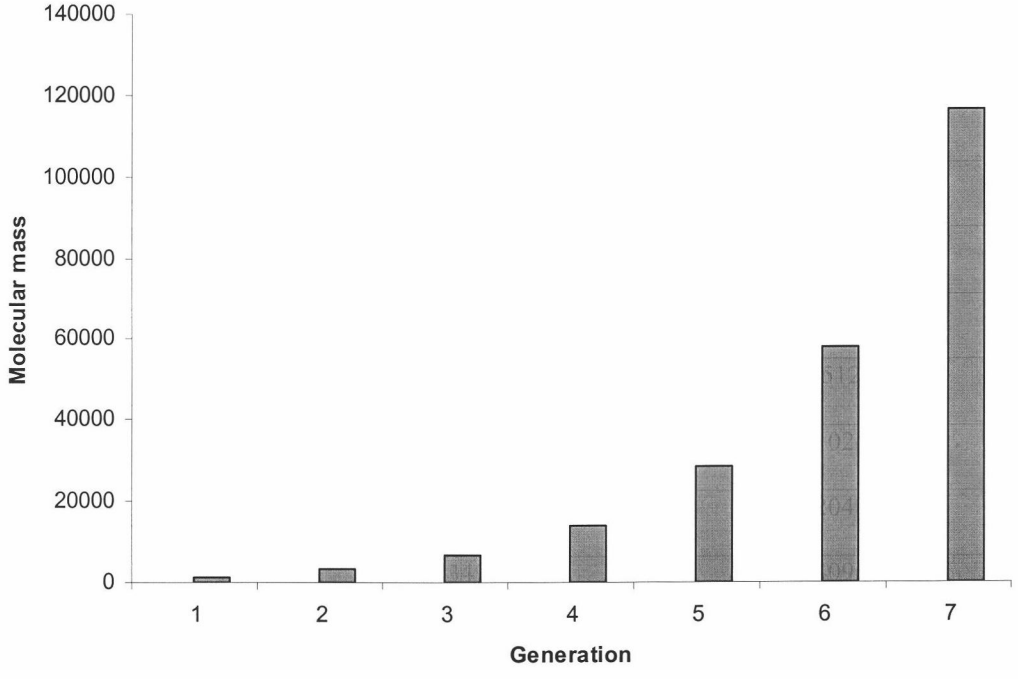

Fig 1.4. Molecular mass of PAMAM dendrimers with EDA core

The molar mass of the dendrimer can be predicted mathematically [5]:

$$M = M_c + n_c.[M_m((n_m{}^G-1)/(n_m-1))+M_t.n_m{}^G] \qquad (1.1)$$

where M_c is the molar mass of the core, M_m is the molar mass of the branched monomer, M_t is the molar mass of the terminal groups, n_c is the core multiplicity, n_m is the branch juncture multiplicity, and G is the generation number.

The increase in the number of dendrimer terminal groups (Z) is consistent with the geometric progression:

$$Z = n_c \, . \, n_m{}^G \qquad (1.2)$$

1.2. Molecular structures

The structure of a generation 2 PAMAM dendrimer is shown in figure 1.5.

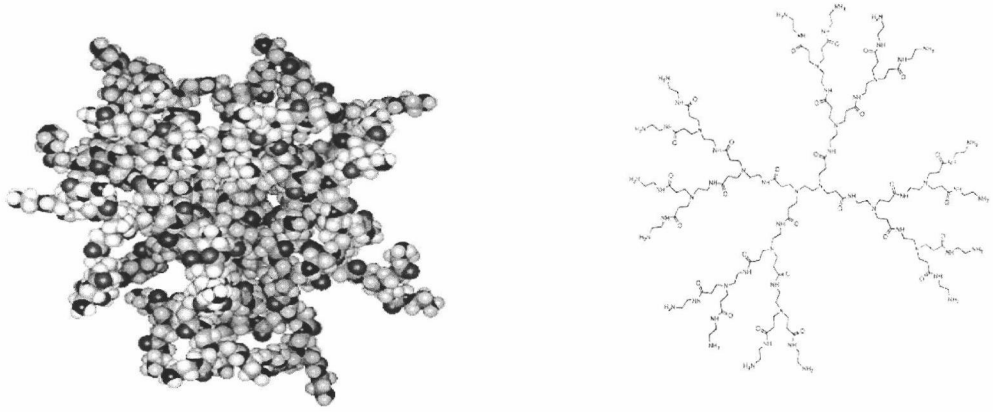

Figure 1.5 (A) Structure of PAMAM dendrimer showing its 3-D-space-filling model, and (B) branched architecture (generation 2) [6]

Compared to higher generations, dendrimers of low generations (generations 1, 2, 3) are more asymmetric and open in structure. Starting at generation 4, as branch density increases with generation, dendrimers are more globular in structure [7]. They become densely packed as they extend out to the periphery, which forms a closed membrane-like structure. They are characterized by the presence of internal cavities and a large number of reactive end groups (figure 1.6).

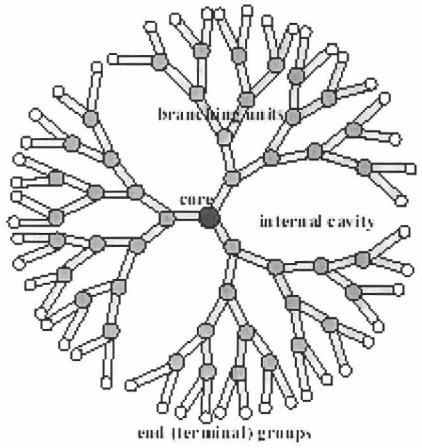

Figure 1.6. Representation of a fourth generation dendrimer [8]

1.3. Properties

Compared to linear polymers, dendrimers show improved physical and chemical properties. Unlike linear polymers, which are random in nature and produces molecules of different sizes, dendrimers are monodisperse macromolecules. The size and molecular masses of dendrimers can be specifically controlled during synthesis.

In solution, dendrimers form a tightly packed ball, which results in a significantly lower viscosity for dendrimers than for similar molecular weight linear polymers [9]. Dendrimers also have high solubility and miscibility, and reactivity, properties owing to the presence of many end-groups [9]. The solubility of dendrimers is strongly influenced by the nature of the surface groups. Dendrimers terminated in hydrophilic groups are soluble in polar solvents, while dendrimers terminated in hydrophobic groups are soluble in nonpolar solvents.

A unique property of dendrimers is the possibility of using them to encapsulate guest molecules in the macromolecule interior. This property arises from their globular shape and the presence of internal cavities. Also notable are their biological properties (discussed later); important because of their growing use in biomedical applications. Of most importance here are PAMAM (amine-terminated) and poly(propyleneamine) dendrimers. These form cationic groups at low pH and are haemolytic and cytotoxic. Their toxicity is generation-dependent and increases with the number of surface groups [10].

1.4. Applications

Dendrimers have great potential in biomedical and pharmaceutical applications, mostly because of their unparallaled molecular uniformity, multifunctional surface, and presence of internal cavities. PAMAM dendrimers have been applied in in vitro diagnostics, in preclinical studies as contrast agents for magnetic resonance [11-14], in the targeted delivery of drugs and other therapeutic agents [15-21], and in gene therapy as carriers, called vectors [22-23].

Examples of such applications are as follows [24]. Dendrimers have been used in in-vitro diagnostics, where dendrimer-antibody conjugates are used for detection of heart damage. Dendrimers are being tested in preclinical studies as contrast agents (paramagnetic metal cations) for magnetic resonance imaging (MRI) to improve sensitivity and specificity of the diagnostic method. Dendrimer have also been used in targeted delivery of drugs, where the drug molecules can be loaded both in the interior of the dendrimers or on the surface. They can also act as carriers for the delivery of genetic materials, such as oligonucleotides or DNA, for gene therapy.

Aside from biomedical applications, dendrimers can also be used for industrial applications. They are useful in environmentally friendly industrial processes; dendrimers have been used to encapsulate insoluble materials, such as metals, and transport them into a solvent within their interior [25]. PAMAM dendrimers have also been used as size standards. The exceptionally uniform molecular size of the various generations of PAMAM dendrimers make them excellent size standards for calibration of analytical instruments.

References

[1] Tomalia, D.A., Baker, H., Dewald, J.R., Hall, M. Kallos, G., Martin, S., Roeck, J., Ryder, J. & Smith, P. *Polym. J.* **1985**, *17*, 117–132.

[2] Ebber, A., Vaher, M., Peterson, J., Lopp, M. *J. Chromatogr. A* **2002**, *949*, 351-358

[3] Hodge, P. *Nature* **1993**, *362*, 18–19.

[4] Alper, J. *Science* . **1991**, *251,* 1562–1564.

[5] Tomalia, D.A., Naylor, A.M. & Goddard III, W.A. *Angew. Chem., Int. Edn.* **1990**, *29*, 138–175.

[6] Dendritech, Inc. Structure of PAMAM dendrimer. www.nmi.org/dendritech/index.html

[7] Caminati, G., Turro, N.J. & Tomalia, D.A. *J. Am. Chem. Soc.* **1990**, *112*, 8515–8522.

[8] Klajnert, B., Bryszewska, M. *Acta Biochimica Polonica*, **2001**, *48*, 199-208

[9] Fréchet, J.M.J. *Science.* **1994**, *263*, 1710–1715.

[10] Roberts, J.C., Bhalgat, M.K. & Zera, R.T. *J. Biomed. Material Res.* **1996**, *30*, 53–65.

[11] Wiener, E.C., Auteri, F.P., Chen, J.W., Brechbiel, M.W., Gansow, O.A., Schneider, D.S., Belford, R.L., Clarkson, R.B. & Lauterbur, P.C. *J. Am. Chem. Soc.* **1996**, *118*, 7774–7782.

[12] Bryant, L.H., Brechbiel, M.W., Wu, C., Bulte, J.W.M., Herynek, V. & Frank, J.A. *J. Magn. Reson. Imaging* **1999**, *9*, 348–352.

[13] Bourne, M.W., Margerun, L., Hylton, N., Campion, B., Lai, J.J., Derugin, N. & Higgins, C.B. *J. Magn. Reson. Imaging.* **1996**, *6*, 305–310.

[14] Fischer, M. & Vögtle, F. *Angew. Chem., Int. Edn.* **1999**, *38*, 884–905.

[15] Twyman, L.J., Beezer, A.E., Esfand, R., Hardy, M.J. & Mitchell, J.C. *Tetrahedron Lett.* **1999,** *40*, 1743–1746.

[16] Liu, M., Kono, K. & Fréchet, J.M.J. *J. Controlled Release 65*, 121–131.

[17] Zhuo, R.X., Du, B. & Lu, Z.R. *J. Controlled Release* **2000**, *57*, 249–257.

[18] Hawthorne, M.F. *Angew. Chem., Int. Edn.* **1993**, *32*, 950–984.

[19] Barth, R.F., Adams, D.M., Soloway, A.H., Alam, F. & Darby, M.V. *Bioconjug. Chem.* **1994**, *5*, 58–66.

[20] Liu, L., Barth, R.F., Adams, D.M., Soloway, A.H. & Reisefeld, R.A. *J. Hematotherapy*. **1995**, *4*, 477–483.

[21] Capala, J., Barth, R.F., Bendayam, M., Lauzon, M., Adams, D.M., Soloway, A.H., Fenstermaker, R.A. & Carlsson, J. *Bioconjug. Chem.* **1996**, *7*, 7–15.

[22] Bielinska, A.U., Kukowska-Latallo, J.F., Johnson, J., Tomalia, D.A. & Baker, J.R. *Nucleic Acids Res.* **1996**, *24*, 2176–2182.

[23] Kukowska-Latallo, J.F., Raczka, E., Quintana, A., Chen, C.L., Rymaszewski, M. & Baker, J.R. *Hum. Gene Therapy* **2000**, *11*, 1385–1395.

[24] Dendritech, Inc. PAMAM dendrimers applications. www.dendritech.com/applications.html

[25] Cooper, A.I., Londono, J.D., Wignall, G., McClain, J.B., Samulski, E.T., Lin, J.S., Dobrynin, A., Rubinstein, M., Burke, A.L.C., Fréchet, J.M.J. & DeSimone, J.M. *Nature* **1997**, *389*, 368–371.

CHAPTER 2

INTRODUCTION TO CAPILLARY ELECTROPHORESIS AND CAPILLARY ELECTROCHROMATOGRAPHY

This chapter describes the basic theoretical concepts and operational principles of capillary electrophoresis (CE) and capillary electrochromatography (CEC). The discussion is intended to provide enough background to understand the basic operation of CE instruments and the principles by which CE and CEC separate analytes. Separations of PAMAM dendrimers using these techniques will be discussed in great detail in chapter 3.

2.1. Introduction to Capillary Electrophoresis (CE)

Electrophoresis is the movement or migration of ions or solutes under the influence of an electric field. In CE, a positive (anode) and negative (cathode) electrode are placed in a solution containing ions. A voltage is then applied across the electrodes causing solute ions of different charge, i.e., anions (negative) and cations (positive) to migrate through the solution across the capillary towards the electrode of opposite charge. Analytes will be separated based on differences in their electrophoretic mobilities, determined by their charge and mass.

Narrow-bore capillaries are employed in CE, typically having an internal diameter (ID) from 25 to 100 μm (375 μm OD). CE offers advantages in the amounts of reagents and samples used given the small size of these capillaries. The

application of high fields (30 kV) allows for rapid analysis time in CE. High separation efficiencies can also be obtained. This technique has been used for a wide range of sample types, such as proteins, oligonucleotides, chiral compounds, surfactants, pharmaceuticals, and environmental samples [1-8].

2.1.1. Instrumentation

The schematic diagram of a basic CE instrument is shown in figure 2.1. It consists of an autosampler, a capillary, two electrodes (cathode and anode) connected to a high-voltage power supply capable of generating up to 30 kV, a detection method, and data acquisition system. Both ends of the capillary are placed in separate buffer reservoirs (inlet and outlet). The sample is introduced into the capillary by applying either electric potential (electrokinetic injection) or pressure (hydrodynamic injection) for usually 1-5 seconds at one end of the capillary (usually the anode). Once the sample is in the capillary, the buffer solution is replaced in the capillary inlet, an electric potential is applied across the capillary, the ionic species in the sample plug will migrate, and the separation is performed. Eventually, the separated analytes will pass through a detector near the opposite end of capillary where information is collected and stored by a data acquisition system.

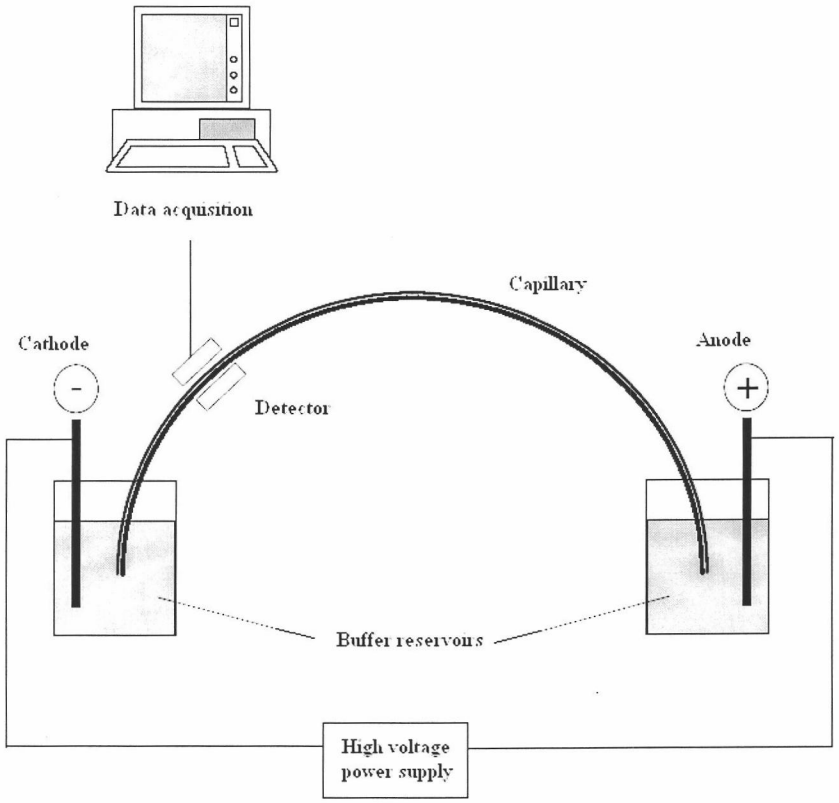

Fig. 2.1. Schematic diagram of a CE system.

2.1.2 Electrophoresis Theory

2.1.2.1 Electrophoretic mobility

To fully understand electrophoresis theory, a basic understanding of electrophoretic mobility is of the utmost importance. Each ion or solute has a finite electrophoretic mobility, and thus separation of mixtures of different ions and solutes in electrophoresis is determined by the differences in their electrophoretic mobility.

Electrophoretic mobility (μ_{ep}) of a charged species can be approximated by the following equation (the Debye-Huckle-Henry theory) [9]:

$$\mu_{ep} = q / (6\pi\eta r) \qquad (2.1)$$

where q is the charge on the ion, η is the viscosity of the buffer and r is the ion radius. From equation 2.1, it is clear that both charge and radius have an effect in electrophoretic mobility. The charge on the ion (q) is affected by the pH of buffer solution, whereas the ion radius (r) can be affected by many factors, such as counter-ion effects, non-spherical shape or other non-ideal behaviors of molecules. Thus, differences in electrophoretic mobility will be caused by differences in the charge-to-size ratio of analyte ions. Since size very closely relates to the mass of the molecule, it is commonly called the "Charge to Mass Ratio". Higher charge and smaller size causes ions to have greater mobility, whereas lower charge and larger size means lower mobility.

Under the same electric field strength, different ions and solutes have different electrophoretic mobilities, and thus they also have different migration velocities (u_{ep}), which can be expressed as [9]:

$$u_{ep} = \mu_{ep} E \qquad (2.2)$$

where u_{ep} is ion migration velocity (ms^{-1}), μ_{ep} is electrophoretic mobility ($m^2V^{-1}s^{-1}$) and E is electric field strength (Vm^{-1}). The electric field strength is a function of the applied voltage divided by the total capillary length. Thus, the actual migration velocity of an ion takes into account the ions individual electrophoretic mobility and the applied voltage.

Electrophoretic mobility is not the only force that drives the movement of analytes in the capillary. If the applied field were the only force acting on the ions, under normal polarity (i.e. inlet (+)-detector-outlet(-)), cations would pass the detector while neutral components will stay at the inlet and anions would be driven away from the detector. Another force, called "electroosmotic flow (EOF)" thus plays a principle role in CE as the bulk flow of liquid through the capillary that will drives all the movements in the capillary toward the detector.

2.1.2.2. Electroosmotic Flow (EOF)

To understand the generation of EOF inside the capillary, Stern's model, as presented in Figure 2.2, is discussed. The inner wall of a fused silica capillary possesses ionizable silanol groups on the surface. During electrophoresis, these silanol groups dissociate to give the capillary wall a negative charge (SiO^-). In contact with buffer solution, this attracts the positively charged ions from the buffer solution, giving rise to electrical double layer. The layer of ions closest to the surface is called the "Stern layer" and is essentially rigid or immobile. A more diffuse layer is formed distal to the Stern layer and is known as the "Gouy layer". This mobile layer is rich in cations and decays into the bulk liquid.

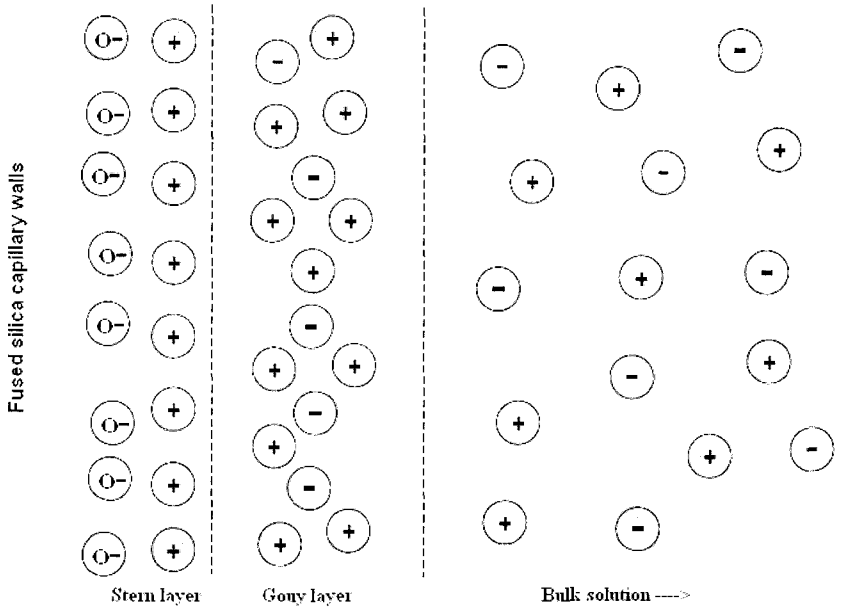

Fig 2.2. Schematic representation of the electrical double-layer at a negatively charged capillary wall.

The formation of electrical double layer gives rise to a potential that falls off exponentially as a function of distance from the capillary surface. The potential drop between the silica wall and the interface of the diffuse layer and bulk solution is called the zeta potential, ζ, with values ranging from 0-100mV. The distance between Stern layer and a point in the bulk liquid at which the potential is 0.37 times the potential at the interface between Stern and diffuse layer, is defined as the thickness of the double layer (δ).

The equation describing δ (the thickness of double layer) was given by Knox [11] as follows:

$$\delta = [\varepsilon_r \varepsilon_o RT/2cF^2]^{1/2} \quad (2.3)$$

where δ= thickness of double layer, ε_r = dielectric constant or relative permitivity of medium, ε_o = permitivity of a vacuum, R = universal gas constant, T = absolute temperature, c = molar concentration, and F = Faraday constant.

Using the above equation, for a monovalent electrolyte at a concentration of 0.001M in water (ε_r = 80), the thickness of the electrical double layer would be 10nm, and at a concentration of 0.1M it would be 1nm.

The zeta potential (ζ) is dependent on δ and the charge density σ as shown in the following equation [12]:

$$\zeta = (\delta\sigma)/(\varepsilon_o \varepsilon_r) \quad (2.4)$$

The relationship between the EOF linear velocity u_{eo} and ζ is given by the Smoluchowski equation as follows:

$$u_{eo} = \varepsilon_o \varepsilon_r \zeta E/\eta \quad (2.5)$$

where ε_o = the permitivity of a vacuum, ε_r = dielectric constant of the eluent, ζ = zeta potential, E = electric field strength, and η viscosity of the solvent.

It is now apparent that the electroosmotic flow depends upon the surface charge density, the field strength, the thickness of the electrical double layer, and

the viscosity of the separation medium which in turn is dependent upon the temperature.

When a voltage is applied longitudinally along the capillary, cations in the diffuse (Gouy) layer are free to migrate toward the cathode, carrying the bulk solution with them. The result is a net flow in the direction of the cathode, known as the electroosmotic flow (EOF).

The main factor affecting EOF mobility is buffer pH. EOF mobility will be significantly greater at high pH compared to low pH. At high pH (pH>9), silanols on the capillary surface are completely ionized and thus, EOF mobility is at its greatest. At low pH (pH<4), however, the ionization of silanols is low and the EOF mobility is insignificant. The ionic strength of the buffer will also affect mobility.

In summary, a solute apparent electrophoretic mobility (μ_x) takes into account both its individual electrophoretic mobility (μ_e) and EOF mobility (μ_{eo}).

$$\mu_x = \mu_{ep} + \mu_{eo} \qquad (2.6)$$

Under normal polarity, samples are introduced at the anode and EOF migrates toward the cathode. In this case, cations have positive μ_{ep}, neutrals have zero μ_{ep}, and anions have negative μ_{ep}. In other words, cations migrate faster than the EOF and anions migrate more slowly than the EOF, whereas neutrals migrate with the same velocity as the EOF. Thus, to determine EOF velocity experimentally, a neutral marker can be injected into the capillary under a given set of conditions

used. By calculating the time that it takes for the neutral marker to reach the detector, EOF can then be determined.

2.1.2.3. Flow Profile in CE

An important characteristic of EOF is its flat flow profile, as opposed to the parabolic or laminar flow profile generated by an external pump used in HPLC, shown in figure 2.3. The generation of a flat profile comes from the evenly distributed charge on the capillary wall, and thus, the flow velocity is uniform across the capillary. This contrasts with pressure-driven flow, such as in HPLC, in which frictional forces at the column walls induce a parabolic or laminar flow profile, which will yield broad peaks due to the dispersive nature of the broad range in flow velocity. With a flat profile, zone broadening is minimized, leading to high separation efficiencies.

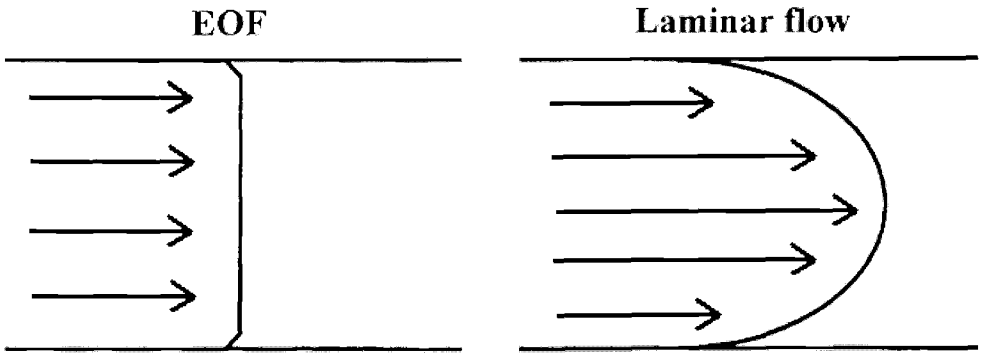

Fig 2.3. Flowprofiles of EOF and laminar flow.

2. 2. Capillary Electrochromatography (CEC)

2.2.1 Introduction to capillary electrochromatography (CEC)

Capillary electrochromatography (CEC) is a hybrid method between capillary HPLC and capillary electrophoresis (CE). It combines the high separation efficiency that CZE offers with the wide range of parameters that HPLC offers, particularly with a wide range of stationary phases to choose from. Subsequently, CEC has become a powerful technique that has gained considerable interest in the last few years.

High efficiencies can be achieved in CEC mainly due to the use of electroosmotic flow (EOF). Consequently, the flow profile created is plug-like, unlike the parabolic flow that HPLC created. Another benefit of using EOF is the usage of small diameter packings (0.5-2μm) due to the absence of column back pressure, and thereby achieving very high efficiencies. In CEC, separations are generally carried out using aqueous buffer in fused-silica capillaries of 25-100μm i.d. packed with small particles (<5μm) in an applied electric field.

CEC was first introduced more than 30 years ago (1974) when Pretorius et al.[13] first demonstrated the ability to use electroosmotic flow in order to drive a mobile phase through a liquid chromatography column. They used 75 to 125 μm particles in a 1 mm i.d. glass tube and were able to show that band broadening with EOF was considerable smaller than with pressure driven flow. In 1981, Jorgenson and Lukacs [14] further proved the principle of electrically driven

chromatography using small diameter particles. Although the efficiencies were relatively low (~60,000 plates/m), they were able to separate 9-methylanthracene from perylene on a 170 μm i.d. capillary packed with 10μm reversed-phase packing material. The work that finally resurrected the interest in CEC, however, was pioneered by Knox and Grant in 1987 and 1991[11,15] with their theoretical and practical approach that demonstrated the feasibility of CEC.

2.2.2 Theory of CEC

As mentioned earlier, EOF-driven chromatography yields higher separation efficiencies than HPLC due to the use of small particles and reduction of plate heights as a result of the plug-flow profile. As discussed in the previous section, the origin of EOF in CZE is the electrical double layer that exists at the liquid – solid interface of a charged surface in contact with an electrolyte solution (fig. 2.4 A). In a capillary packed with silica particles, the surface of both the capillary wall and of the particles are negatively charged due to the dissociation of silanol groups (fig. 2.4 B). In fact, the surface areas of silica based packing materials are much greater than that of the capillary wall, thus most of the EOF is generated by the surface silanol groups of the stationary phase. When an axial electrical field is applied to the column, ions in the diffuse section of the double layer migrate towards the cathode moving the bulk solution by viscous drag.

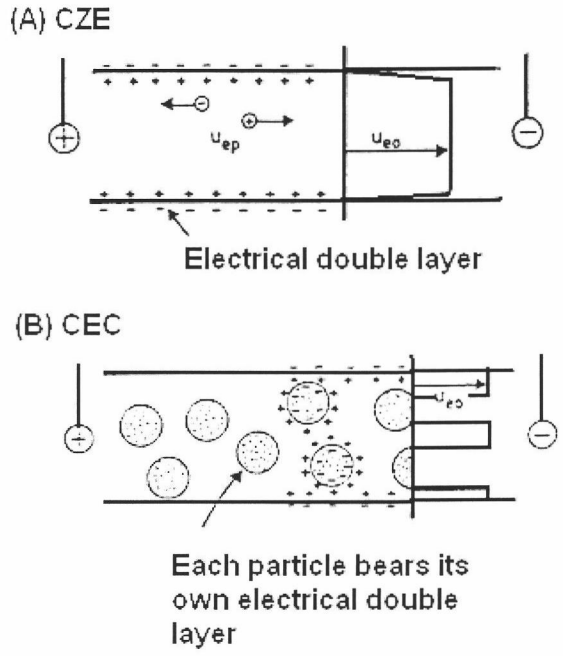

Fig 2.4. Schematic representation of (A) CZE, and (B) CEC inside a capillary column [19].

The linear velocity in a pressure driven system is given by the following equation described by Knox and Grant [6]:

$$u = d^2 \Delta p / (\Phi \eta L) \qquad (2.7)$$

where u = linear velocity, d = particle diameter, Φ = pressure resistance factor for packed columns, Δp = pressure drop across the column, L = column length, η = viscosity of the solvent.

On the other hand, the linear velocity through a packed capillary under an applied electric field is given by the Smoluchowski equation, as discussed above:

$$u = \varepsilon_o \varepsilon_r \zeta E / \eta \qquad (2.5)$$

where ε_o = the permitivity of a vacuum, ε_r = dielectric constant of the eluent, ζ = zeta potential, E = electric field strength, and η = viscosity of the solvent.

When comparing these 2 equations, you can see that the linear velocity u is proportional to d^2 in a pressure driven system while it is independent of the particle diameter in an electrically driven system. Since plate values are generally lowered as a result of using small diameter particles, thus, it is possible in electrically driven system to use very small diameter packing materials and still maintain high linear velocities to yield rapid and very efficient separations.

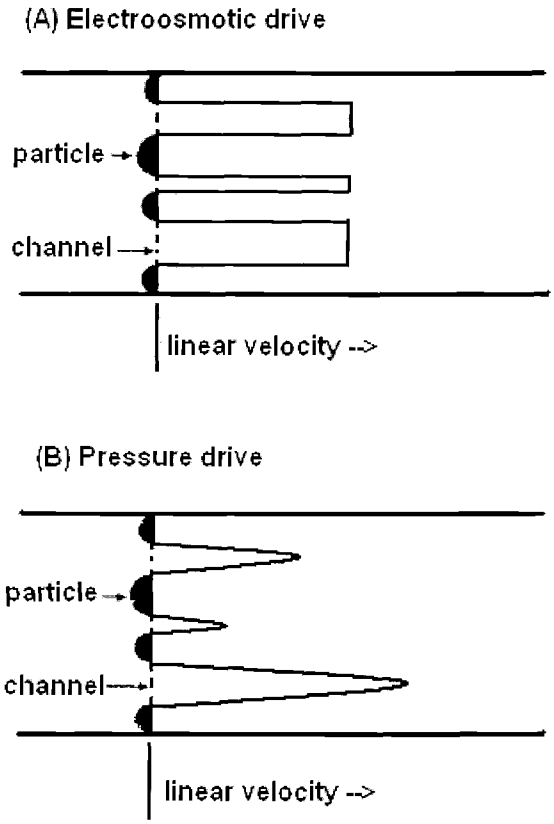

Fig. 2.5. Schematic representation of (A) electroosmotic, and (B) pressure-driven flow in a CEC packed column

2.2.3. CEC Instrumentation

The instrument used for CEC is the same in principle as a CZE instrument. The only modification from a conventional CE system is the pressurization of the solvent reservoirs. Both inlet and outlet ends of the capillary column need to be pressurized in order to prevent bubble formation.

2.3. Monolithic columns

The packing in a CEC column plays an important role in providing sites for the required interactions as in HPLC as well as in creation of EOF, the development of both (1) specific particulate packings having properties tuned for CEC, as well as (2) alternative column technologies, is emerging.

Packed capillary columns have been successfully used in CEC separations as has been demonstrated in numerous papers [16-18]. The preparation of these columns includes the fabrication of retaining frits within a capillary and the packing of small diameter particles into narrow-bore capillaries. However, both these steps present technical difficulties associated with packing and retaining beads in narrowbore columns, and thereby reproducibility of this procedure remains problematic.

These limitations have led to the development of various alternative approaches. Fritless monolithic columns, in particular, which emerged during the last decade [20-28], have proven to be a viable alternative to packed capillary CEC. They prepared from insitu polymerization to form a continuous porous bed. Monolithic columns have special characteristics and present several advantages, mainly in their ease of their preparation [29-31].

These advantages include: 1) the polymerization process is simple and can be performed directly within the confines of a capillary or a microfluidic chip, thus avoiding the problems related to both frit formation and packing, 2) columns of virtually any length and shape can be fabricated, 3) the polymerization mixture can

be prepared using a wide variety of monomers, allowing a nearly unlimited choice of both matrix and surface chemistries, 4) the polymerization process can be easily controlled which enables optimization of the porous properties of the monolith, and consequently the flow rate and chromatographic efficiency of the system.

Polymeric monolithic columns have been widely developed and successfully applied for CEC. As can be seen from fig.2.6, the preparation of monolithic porous polymer sorbent is a simple and straightforward process. The steps consist of: 1) the modification of the capillary wall in order to provide functional groups on the surface that will participate in the subsequent polymerization process, 2) filling the capillary with the homogeneous polymerization mixture consisting of the monomers, initiator, and porogenic solvent, 3) the initiation of polymerization by temperature of UV radiation to obtain a rigid monolithic porous polymer, and 4) the removal of the unreacted components, such as the porogenic solvents and any other soluble compounds that remain in the polymer.

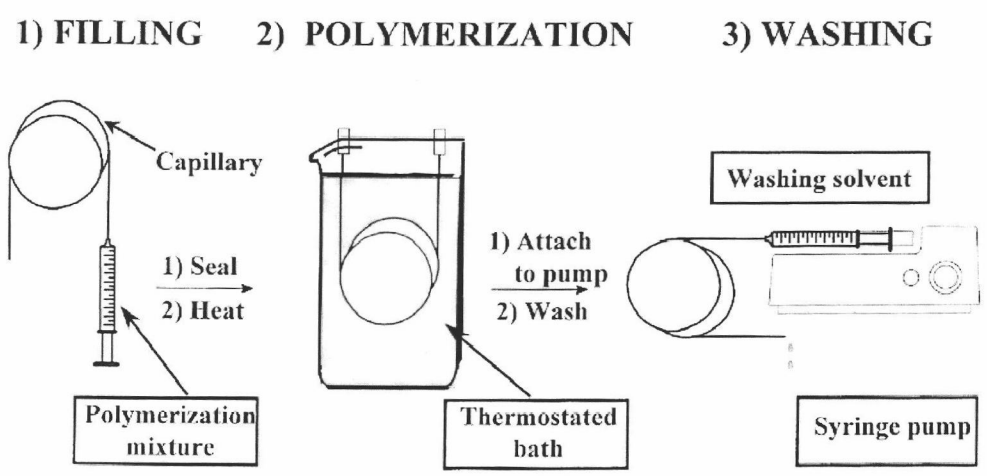

Fig 2.6. Schematic representation of the preparation of a monolithic column [32]

As mentioned before, a large number of available monomers with a wide variety of functionalities are available giving unlimited choices of surface chemistry. They may be used directly for the preparation of polymer monoliths and some are shown in fig.2.8.

(A) Monomers

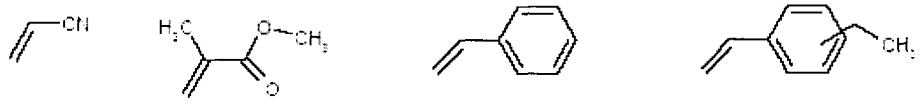

acrylonitrile (AN) methyl methacrylate (MMA) styrene ethylstyrene

(B) Cross-linkers

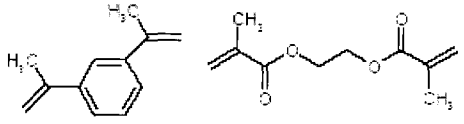

1,3-diisopropenyl benzene (DIP) ethylene glycol dimethacrylate (EGDMA)

(C) Charged monomer for EOF generation

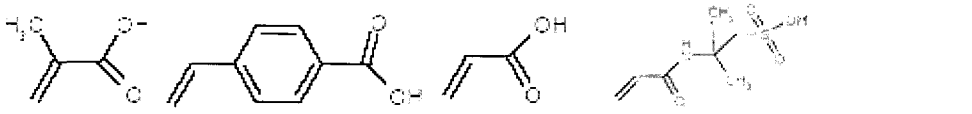

methacrylic acid (MAA) *p*-vinylbenzoic acid acrylic acid (AA) acrylamido-(2-methyl)-propane sulfonic acid (AMPS)

(D) Initiators

azobisisobutyronitrile 2,2-dimethoxy-2-phenyl-acetophenone

Fig. 2.7. Selection of (A) monomers with functional groups, (B) cross-linkers, (C) charged monomers for EOF generation, and (D) chemical initiators used for the preparation of polymer monolithic columns.

References:

[1] Altria, K.D, Bryan, S.M, Hadgett, T.A., *J.Pharm. Biomed. Anal.* **1997**, *15*, 1091-1101

[2] Chee, G.L, Wan T.S.M., *J. Chromatogr*, **1993**, *612*, 172-177

[3] Altria, K.D., Chanter, Y.L., *J Chromatogr A*, **1993**, *652*, 459-463

[4] Gilpin, R.K, Pachla, L.A, *Anal. Chem*, **2003**, 75R

[5] Shafaati, A, Clark, B.J. *Analytical Proceedings*, **1993**, *30,* 481-483

[6] Landers, J.P, Ed., *Handbook of Capillary Electrohoresis*, CRC Press, Boca Raton, **1997**

[7] Monnig, C.A., Kennedy, R.T. *Anal Chem* **1994**, *66,* 280R-314R

[8] Thorman, W., Molteni, S., Caslavska, J., Schmutz, A, *Electrophoresis*, **1994,** *15*, 3-12

[9]Jorgenson, J.W., Lukasc, K.D. *Anal Chem* **1981**, *53*, 1298

[10]Remcho, V.T., *Chem. Educator*, **1997**, *2*

[11] J.H. Knox and I.H. Grant, *Chromatographia*, **1987,** *24*, 135-143.

[12] Shaw, D.J. *Electrophoresis*. Academic Press, London, **1969**

[13] V. Pretorius, B.J. Hopkins and J.D. Schieke, *J. Chromatogr.* **1974**, *99*, 23-30

[14] J. Jorgenson and Lukacs, *J. Chromatogr.*, **1981**, *218*, 209-216

[15] J.H. Knox and I.H. Grant, *Chromatographia*, **1991**, *32*, 317 - 327

[16] Colón, L. A., Burgos, G., Maloney, T. D., Cintron, J. M., Rodriguez, R. L., *Electrophoresis* **2000**, *21*, 3965–3993.

[17] Vanhoenacker, G., Van den Bosch, T., Rozing, G., Sandra, P., *Electrophoresis* **2001**, *22*, 4064–4103.

[18] Cikalo, M. G., Bartle, K. D., Robson, M. M., Myers, P., Euerby, M. R., *Analyst* **1998**, *123*, 87R-102R.

[19] J.H. Knox, *Chromatographia* **1988**, *26*, 329–337.

[20] S. Hjerten, D. Eaker, K. Elenbring, C. Ericson, K. Kubo, J.L.Liao, C.M. Zeng, P.A. Lindstr_m, C. Lindh, A. Palm, T. Srichiayo,L. Valcheva, R. Zhang, Jpn. J. *Electrophoresis* **1995**,*39*, 105.

[21] E.C. Peters, M. Petro, F. Svec, J.M.J. Frechet, *Anal. Chem.* **1997**, *69*, 3646–3649.

[22] A. Palm, M.V. Novotny, *Anal. Chem.* **1997**, *69*, 4499–4507.

[23] L. Schweitz, L.I. Andersson, S. Nilsson, *Anal. Chem.* **1997**, *69*, 1179–1183.

[24] M.T. Dulay, R.P. Kulkarni, R.N. Zare, *Anal. Chem.* **1998**, *70*, 5103–5107.

[25] I. Gusev, X. Huang, C. Horv_th, *J. Chromatogr. A* **1999**, *855*, 273–290.

[26] G. Chirica, V.T. Remcho, *Electrophoresis* **1999**, *20*, 50–56.

[27] Q.L. Tang, B.M. Xin, M.L. Lee, *J. Chromatogr. A* **1999**, *837*,35–50.

[28] N. Tanaka, H. Nagayama, H. Kobayashi, T. Ikegami, K. Hosoya, N. Ishizuka, H. Minakuchi, K. Nakanishi, K. Cabrera, D. Lubda, *J. High Resol. Chromatogr.* **2000**, *23*, 111–116.

[29] Monolithic Materials: Preparation, Properties, and Applications (Eds.: F. Svec, T. B. Tennikova, Z. Deyl). Elsevier, Amsterdam, **2003**.

[30] F. Svec, *J. Sep. Sci.* **2004**, *27*, 747–766.

[31] D. Allen, Z. El Rassi, *Electrophoresis* **2003**, *24*, 3962–3976.

[32]Svec, F., Peters, E.C, Sykora, D, Frechet, J.M.J. *J of Chromatography A* **2000**, *887*, 3-29.

CHAPTER 3

SEPARATIONS OF POLYAMIDOAMINE (PAMAM) DENDRIMERS

Abstract

Starburst polyamidoamine (PAMAM) dendrimers of different generations were analyzed using capillary zone electrophoresis (CZE), capillary electrochromatography (CEC), and high-performance liquid chromatography (HPLC). In this study, PAMAM dendrimers were used as template molecules for preparing porous monolithic polymer sorbents for CEC. The molecules were incorporated into a solution of functionalized monomers, cross linkers, solvent, and initiator. Thermal polymerization, followed by the removal of the solvent and dendrimers, produced a continuous rod of polymer with uniform porosity and controlled surface chemistry. Separations of dendrimers from various generations, as well as from several side products were achieved using CZE, CEC, and HPLC.

3.1 Introduction

Since the pioneering work of Tomalia et al. [1, 2] in 1985, the synthesis and application of dendritic macromolecules have been of significant interest. Applications of dendrimers have included a wide range of areas, such as in *in vitro diagnostics*, in preclinical studies as *contrast agents* for magnetic resonance [3-6], in the targeted *delivery of drugs* and other therapeutic agents [7-13], and in *gene therapy* as carriers [14-15].

Along with these advances in biomedical research, the separation and identification of dendrimers is becoming increasingly important. This is particularly necessary for assessing impurities, as incomplete reaction steps and side reactions may occur during dendrimer synthesis, leading to the formation of byproducts and defective products [16].

A wide variety of analytical techniques have been used in order to characterize PAMAM dendrimers, including UV-vis, Fourier transform infrared (FTIR), NMR, potentiometric titration [17-19], scattering methods [20], capillary electrophoresis [16, 21-24, 47-48], size exclusion chromatography (SEC) [19], HPLC [25-27], electrospray ionization (ESI), matrix-assisted laser desorption ionization time-of-flight (MALDI-TOF), and fast atom bombardment (FAB) mass spectrometry [28-30].

Despite the numerous techniques, separation of various dendrimers still offers challenges, particularly with increasing size of dendrimers. This has prompted research into establishing or refining separation techniques for fast and reliable dendrimer analysis. The aim of the present study was therefore to apply different techniques for the separation of different generations and for the isolation of impurities from individual generations of EDA-core PAMAM dendrimers.

Capillary electrophoresis (CE) has been an increasingly important tool for the analysis of biologic macromolecules, such as DNA [31], protein [32], peptides [33], etc. Separations of different generations of dendrimers are possible mainly due to the nature of PAMAM dendrimers, which carry multiple charges. Thus, they can be analyzed by electrophoretic methods since separation in CE does not

depend on the mass of the molecule alone, but rather its charge-to-mass ratio. Additionally, CE offers several advantages, such as high efficiency and sensitivity, short run time, and high automation capability that can be used for fast and quantitative analysis. Routine analysis of dendrimers using CE is then feasible; however, only a limited number of reports can be found in the literature on the analysis of dendrimers using CE [16, 21-24].

In addition to CE, capillary electrochromatography (CEC) is also an important tool in the area of analytical separations. High separation efficiency can be achieved for CEC due to the plug flow profile of the mobile phase, leading to decreased zone broadening. Monolithic columns have developed as an alternative approach to conventional packed columns for LC and CEC. The simple in situ polymerization process performed directly within the confines of a mold avoids the problems associated with frit production and irreproducible packing.

Recently, our research group has developed a new class of porous polymer monoliths for use in LC and CEC that gives control over porosity and the surface chemistry of the sorbent [34]. Uniform pore structures can be generated with porosity controlled not only by adjusting the amount and nature of the porogenic solvent or by incomplete polymerization, but also by adjusting the amount the macromolecular (dendrimer) template.

The procedure involves incorporating the dendrimer into a solution of functionalized monomers, cross linker, solvent, and polymerization initiator. Thermal polymerization, followed by the removal of solvent and dendrimers,

produces a continuous rod of polymer with uniform porosity and dendrimer-influenced surface characteristics.

In the present study, dendrimers were utilized as template molecules for preparing porous monolithic sorbents for CEC (Fig. 3.1). This method provides two advantages: 1) dendrimers can be used as template molecules for controlling pore structures, 2) selective sorbents can be produced with surface sites that are complementary in chemical functionality to the dendrimer template molecule. These highly selective monolithic columns were used for separations of various generations of dendrimers as well as separations impurities from dendrimer products in the CEC mode.

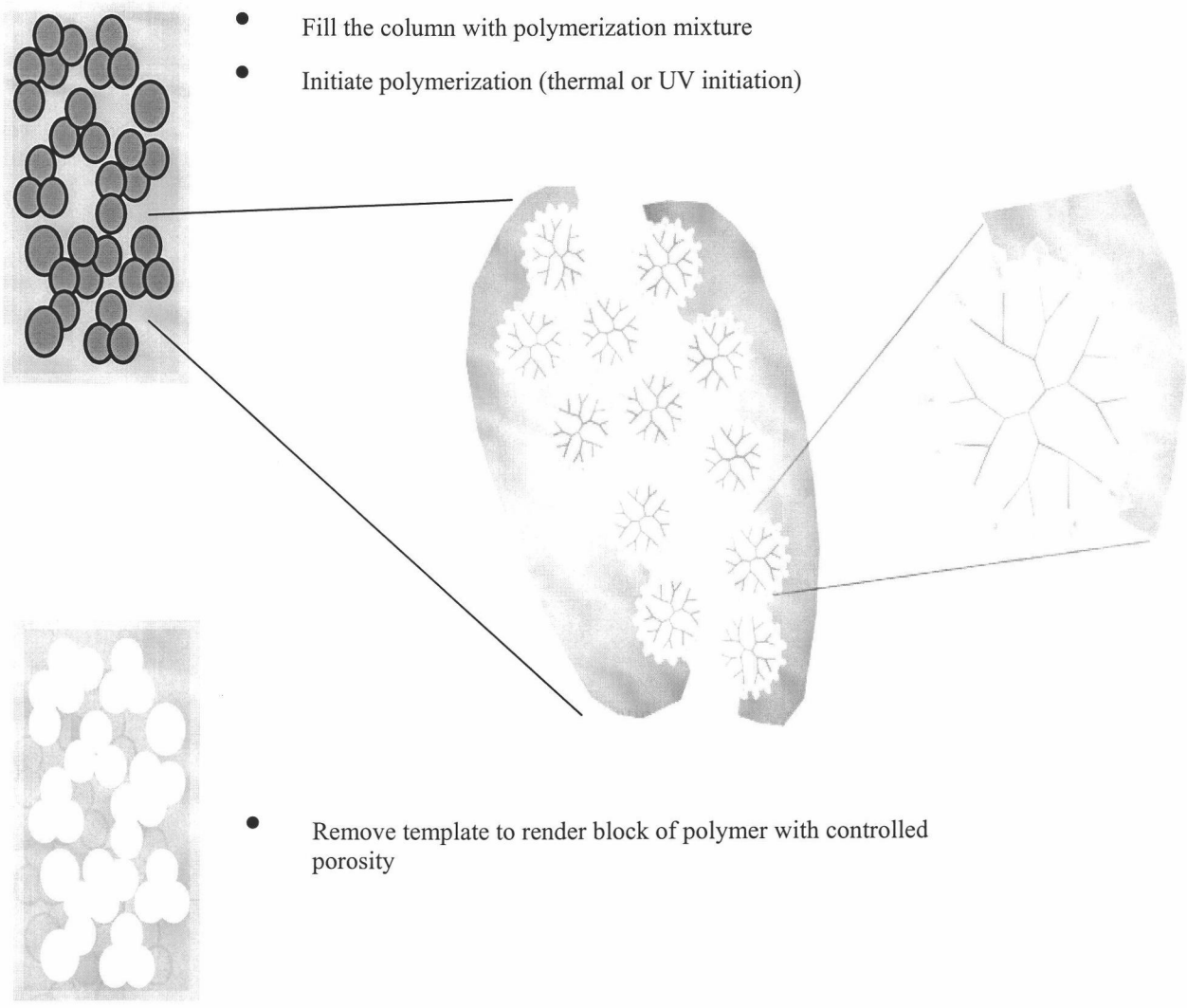

Fig 3.1. General concept for polymer monoliths with macromolecule-templated porosity

Another technique was explored in this study is high-performance liquid chromatography (HPLC), as it is a widely accepted methodology in chemical laboratories for separation and purification of macromolecules. Thus, analysis of dendrimers using HPLC is possible for fast and reliable routine analysis of these macromolecules. Only a limited number of reports on the use of HPLC as a characterization technique for the identification and separation of PAMAM dendrimers are found in the literature [25-27], and this study was intended to provide an alternative over the existing methodology.

In summary, the specific objectives of this study were as follows:

1) To separate various generations of dendrimers, and isolate impurities resulting from incomplete reactions and side reactions occurring during synthesis, for higher purity products. For this study, CE was employed for generational separation of dendrimers as well as separations of impurities separations from the synthesized dendrimers. Applications of this method to microchip CE are discussed in the next chapter.
2) To utilize dendrimers as template molecules for preparing porous monolithic sorbents in CEC for the generation of highly selective sorbents. This approach is particularly critical for higher generation dendrimers as generational separation of dendrimers with high molecular masses still poses problems.
3) To provide an alternative method and ensure the effectiveness of HPLC for detecting and separating various generations PAMAM dendrimers.

3.2 Experimental

3.2.1 Chemicals

Starburst PAMAM dendrimers of different generations with EDA core (5-20% solution in methanol) were purchased from Aldrich (Milwaukee, WI, USA). butyl methacrylate (BMA), methacrylic acid (MAA), ethylene dimethacrylate (EDMA), 2-acrylamido-2-methyl-propanesulfonic acid (AMPS), 2,2'-azobisisobutyronitrile (AIBN), chlorotrimethylsilane, and [(methacryloxy)-propyl] trimethoxysilane were purchased from Aldrich (Milwaukee, WI, USA) and used as received. The solvents (acetonitrile, methanol) were HPLC grade and were purchased from Fisher Scientific (Pittsburgh, PA, USA). Fused silica tubing of 75 μm ID x 360 μm OD was purchased from Polymicro Technologies, Inc. (Phoenix, AZ, USA).

3.2.2 Procedures

3.2.2.1 Capillary Zone Electrophoresis (CZE)

CZE separations of Starburst dendrimers were performed on a HP 3D CE system (Waldbronn, Germany), and a fused silica capillary with an ID of 75 μm, total length of 58.5 cm, and effective length (length to the detection window) of 50 cm. Data acquisition and processing were performed with the Agilent Chem Station software. UV detection was at 200 nm. The full generation dendrimers were analyzed in pH 2.7 50mM phosphate buffer, whereas the half-generations were analyzed in a 20 mM phosphate buffer (pH = 7.8). The sample concentration was 1 mg/mL in buffer solution (and was immediately run after dissolving).

Samples were injected hydrodynamically at constant pressure at 50 mbar for 5 sec, and separations were performed at an applied voltage of 20 kV at 40°C. The influence of sample injection mode (hydrodynamic versus electrokinetic injection) have been compared on the electropherograms of PAMAM dendrimers and the results were unaffected by the two modes of injection. Thus, for this present study, hydrodynamic (pressure) injection was used.

The procedure of analysis was similar to that reported elsewhere [16, 17] with some critical adjustments. Before initial use, the uncoated fused-silica capillaries were flushed with 0.1 M NaOH for 15 min, washed with deionized water for 15 min, and then conditioned with the running buffer for 15 min. Before each injection, the capillary was flushed with 0.2 M H_3PO_4 (5 min) solution, then with 0.1M NaOH (5min), followed by deionized water (5 min), then with the running buffer (5 min).

Some of the capillaries were silanized to study the effect of dendrimer adsorption on the silica surface, and was done as follows [17]. First, the bare fused-silica capillary was pretreated by flushing it with a 1.0 M NaOH solution [49, 50] (30 min) to activate the hydroxyl groups on the silica surface, followed by deionized water (30 min), methanol (30 min), and THF (20 min). The internal wall of the capillary was silanized by filling up the capillary with chlorotrimethylsilane (0.1M in THF) for 24 h. The capillary was extensively flushed using THF (at least 20 min), followed by deionized water, and then equilibrated with the running buffer. Flushing was performed at room temperature.

3.2.2.2 Capillary electrochromatography (CEC)

Electrochromatographic experiments were performed with an HP 3D CE system (Waldbronn, Germany), modified such that pressure of up to 12 bar can be applied on the inlet and/or outlet vials. Data acquisition and processing were performed with the Agilent Chem-Station software. The capillary was equilibrated with the mobile phase (50 mM phosphate buffer) until a stable current and baseline were achieved. Samples were injected electrokinetically (5 kV for 3 s), and separations were performed at an applied voltage of 20 kV at 30°C.

During monolith preparation, the capillaries were examined using a Stereomaster optical microscope (Fisher Scientific, Houston, TX, USA) with 40x magnification. The column morphology was studied using an AmRay (Bedford, MA, USA) scanning electron microscope (SEM) operated at 10 kV.

3.2.2.2.1 Pretreatment of capillaries

For functionalization of the capillary surface, a fused silica capillary (30 cm, 75 um ID, 360 um OD) was derivatized with [(methacryloxy)-propyl] trimethoxysilane solution. The procedure was based on Hjerten's method [35]. First, the capillary was flushed with 1M NaOH solution (at least 30 minutes), followed by H_2O (at least 30 minutes), and finally filled with a solution of 300 µL of [(methacryloxy)-propyl] trimethoxysilane in 1 ml acetone. The solution was kept in capillary for at least 1 hour. The capillary was then flushed with H_2O for 10 minutes and finally emptied and dried with a flow of Nitrogen.

3.2.2.2.2 Preparation of monolithic capillaries

The preparation of monolithic capillaries is diagrammed in fig 3.2. At first, AIBN (1 wt. % with respect to the monomers) was dissolved in a monomer mixture consisting of EDMA (40 wt. %), BMA (59.7 wt. %), and AMPS (0.3 wt. %). Porogenic solvent, methanol (60 wt. %), was then slowly admixed to the monomers in 40:60 (monomer: solvent, v/v). This was the polymerization mixture used for monolithic column preparation.

To prepare the dendrimer-templated monolithic column, Starburst (PAMAM) dendrimer (commercially available as 5-20% solution in methanol) was prepared at several concentrations in a glass vial, and then the solution was allowed to evaporate to remove the methanol. A known volume of monomer polymerization mixture prepared above was then added to the vial to yield the desired dendrimer template concentration. The mixture was then purged with nitrogen for 10 minutes.

The derivatized capillary was filled with this mixture using a 100 μL syringe, and sealed at both ends with rubber septum. Polymerization was carried out by submerging the capillary in a 60°C bath for 20 hours. The resulting monolith was subsequently flushed with mobile phase using a syringe pump to remove the residual reagents, dendrimers, and methanol. Finally, a detection window was burned on a fused silica capillary, and was joined to the monolithic column using a small piece of PTFE tubing.

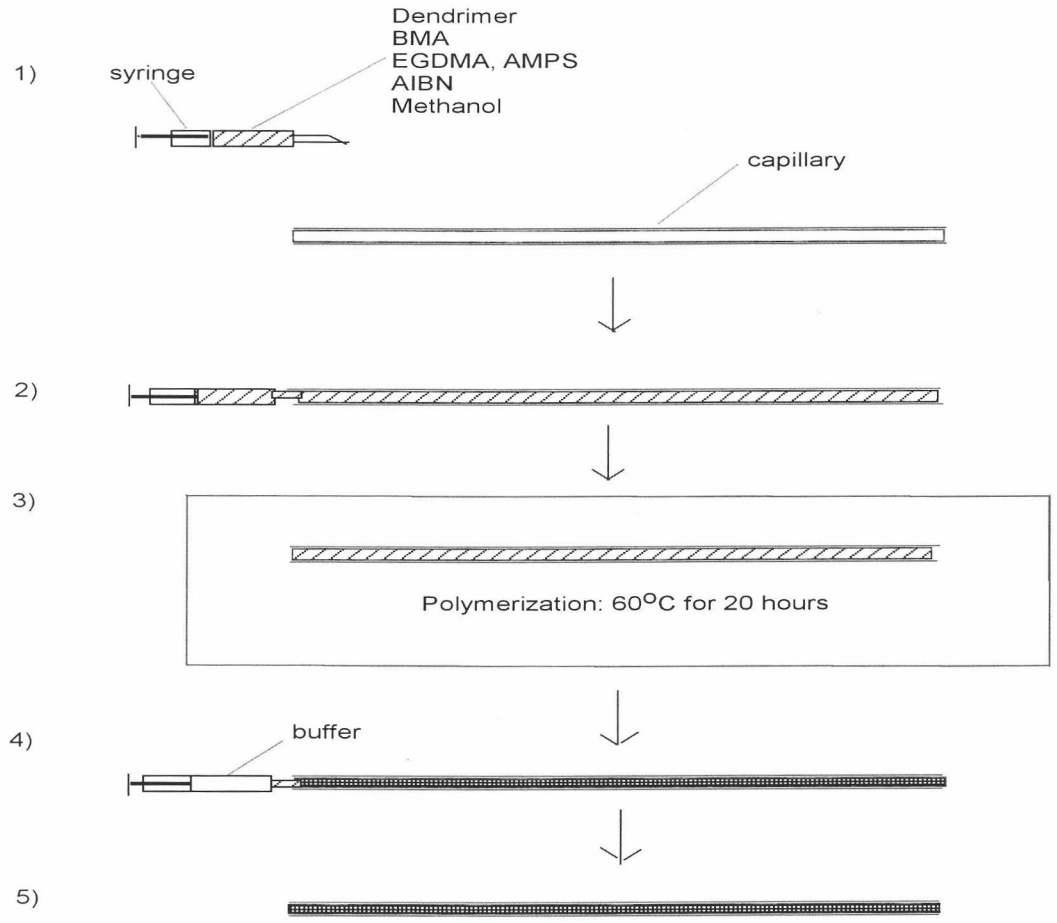

Fig. 3.2. Preparation of dendrimer-templated monolithic sorbents. 1) Prepare a polymerization mixture consists of: PAMAM dendrimer (imprint molecule), EGDMA (crosslinker), BMA (functional monomer), AMPS, AIBN (radical initiator), methanol (porogenic solvent), 2) Fill a capillary derivatized with [(methacryloxy)propyl]-trimethoxysilane with the mixture using a syringe, 3) The polymerization is performed under a water bath for 20 hr at 60^0C, 4) Flush remaining monomers and dendrimer out of the capillary. A detection window is burned on a fused silica capillary open tube, and is joined to the monolithic column using a small piece of PTFE tubing (not shown in picture), 5) The column is now ready for use in CEC

For the preparation of dendrimer-templated monolithic capillary columns with varying type and amount of monomers composition, polymerization mixtures were prepared by mixing monomers, cross-linking monomers (EGDMA), template molecules, and radical initiator (1% wt. AIBN with respect to monomers) in the porogenic solvent methanol with a ratio of 2:3 (v/v) monomers: porogen according to table 3.1. The mixtures were then polymerized in the capillary following the procedure as described in fig. 3.2.

Monolithic column	Template	Monomer (mmoles)		
		BMA	MAA	EGDMA
A	200 µmol G5	8	0	8
B	200 µmol G5	6	2	8
C	200 µmol G5	4	4	8

Table 3.1 Monomers composition for dendrimer-templated monolithic column preparation

3.2.2.3 High Performance Liquid Chromatography (HPLC)

Reverse-phase (RP) HPLC separations were performed on an Agilent 1100 series system (Waldbronn, Germany), consisting of an Agilent 1100 pump and UV detector. Data were collected using Agilent ChemStation software. A reverse-phase Beckman Ultrasphere C-8, 5µm, 4.6mmx 25 cm HPLC column was used. A mobile phase of 80:20 H_2O/0.1%TFA : ACN/0.1%TFA at a flow rate of 0.2 mL/min at 25°C was used. Trifluoroacetic acid (TFA) at 0.1 wt % concentration in water as well as in ACN was used as a counterion to lessen the adsorption of

dendrimer to the stationary phase. The stability of the PAMAM dendrimers in 0.14% aqueous solutions of TFA has been confirmed [26]. Samples were injected into the column through a 20-μl sample loop, and were analyzed at an absorbance of 200 nm and sample concentration of 1 mg/mL.

3.3. Results and discussion

3.3.1 Separations by capillary zone electrophoresis (CZE)

3.3.1.1 Capillary electrophoresis of amine-terminated PAMAM dendrimers

Separations of various generations of amine-terminated dendrimers were conducted in acidic (pH 2.7) conditions. Figure 3.3 shows the CZE separation of EDA-core PAMAM dendrimers, generations 2, 4, and 5, in phosphate buffer solution. The sample was shown to be a complex mixture consisting of three main dendrimer peaks of the generations analyzed having different electrophoretic mobilities. Similar results were obtained for the separation of PAMAM dendrimers in acetate buffer solution at the same pH. Increasing pH to above 3 did not result in any separation. Thus, pH is apparently the predominant factor that affects separation of PAMAM dendrimers. Results have shown that pKa of the terminal primary and tertiary amine groups of PAMAM dendrimers is between 9 and 10, and between 4 and 5, respectively [2,36]. Thus, the low pH condition ($pH < 3.0$) is necessary to have all the terminal amino groups in a PAMAM molecule protonated for separations between full generation dendrimers in CZE to occur.

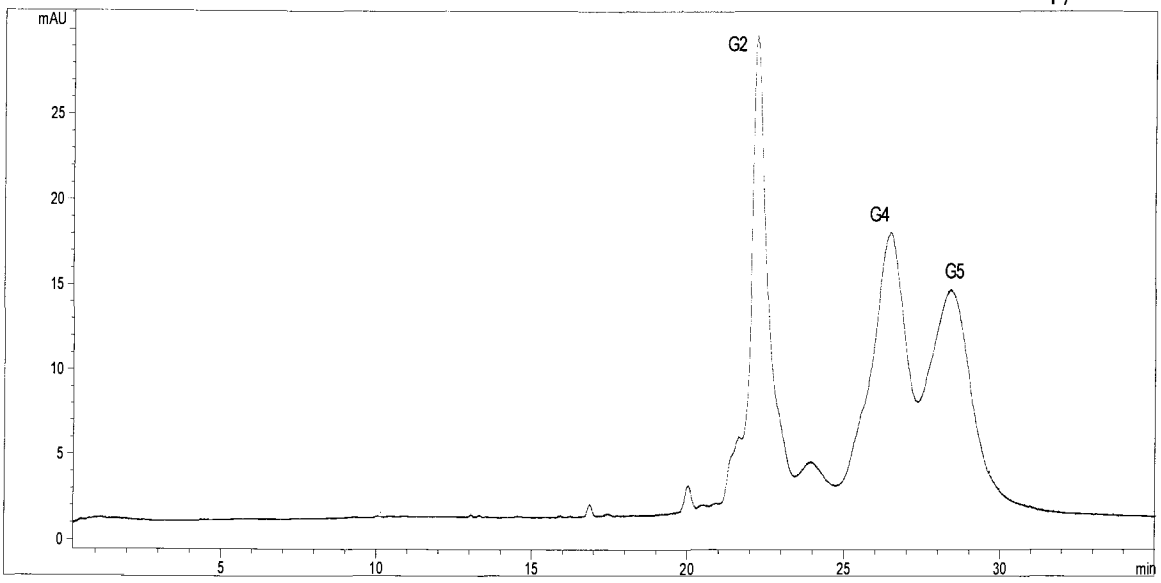

Fig. 3.3 Electropherogram of generation 2, 4, and 5 Starburst dendrimers. Conditions: capillary column, 75 μm ID x 360 μm OD x 50 cm (effective length); 20 kV applied voltage; UV detection at 200 nm; mobile phase, 0.05M phosphate buffer pH 2.7.

Dendrimer	G2	G4	G5
Mr[a)]	3256	14215	28826
Diameter[a)] (nm)	2.9	4.5	5.4
No. of NH_2 groups[a)]	16	64	128
Total no. of N ligands[a)]	30	126	254
Charge/Mr ratio[b)]	0.009214	0.008864	0.008811
Mr[c)]	3185	12910	27250
Average no. of -NH_2 groups[c)]	11.9	46.3	120
Total average no. of –N= ligands[c)]	21.1	98.3	238
Charge/Mr ratio[c)]	0.00662	0.00761	0.00873

Table 3.2 Molecular characteristics of amine-terminated EDA core PAMAM dendrimers [19]
a) Theoretical values
b) Assuming theoretical values and full protonation [37]
c) Practical values determined from titration and GPC measurements

As discussed in the previous chapter, separation in CZE occurs when analytes are charged and have different apparent electrophoretic mobilities (separations are according to the charge-to-mass ratio). As can be seen from eq. 2.1, the charge on the ion is essentially affected only by the pH of buffer solution, whereas the ion radius can be affected by many factors, such as counter-ion effects, non-spherical shape or other non-ideal behaviors of molecules. Therefore, it is understandable that half- and full generations of PAMAM dendrimers must possess different electrophoretic mobilities depending on the pH of the running buffer. In the case of full-generations, the terminal amino groups become protonated in an acidic medium and the electrophoretic mobility of positively charged molecules is in the direction of the electroosmotic flow (towards the cathode).

What makes the separation of PAMAM molecules more complex is that the calculated charge-to-mass ratio between different generations remains essentially constant (assuming the protonation of all amino groups) and therefore, PAMAM dendrimers should have similar electrophoretic mobilities due to the nearly constant value of their charge/mass ratios based on both theoretical calculations and practical measurements (see Table 3.2). The charge to mass ratio values of amine-terminated PAMAM dendrimers range from 0.0066 - 0.0087 based on the acid-base titration and GPC data [17].

Nevertheless, as results in fig. 3.3 show, in an acidic phosphate buffer, where the electroosmotic flow is heavily suppressed (and therefore analyte

electrophoretic mobility is the only transport factor), different generations of EDA-core PAMAM dendrimers are separated. Similar results were also reported by other researchers for separation of PAMAM dendrimers with CZE using bare fused-silica capillaries [16, 17].

A complex mechanism then has to be considered for the mobility of PAMAM dendrimers toward the cathode as can be seen from equation 3.1 in dimensionless form [38].

$$\mu_{ep}' = (\mu_{ep} 3\eta e / 2\varepsilon_0 \varepsilon_r kT)$$

$$= (lL / V t_m)(3\eta e / 2\varepsilon_0 \varepsilon_r kT) \qquad (3.1)$$

where l is the effective length, L is the total length, V is the voltage, t_m is the migration time, μ_{ep} is the electrophoretic mobility, ε_r is the dielectric constant of water (80.5), ε_o is the dielectric permittivity of the vacuum, k is the Boltzman constant, T is the temperature, η is the viscosity and e is charge of the electron.

Based on equation 3.1, the electric field and the hydrodynamic force affect the mobility of PAMAM dendrimers toward the cathode. As discussed earlier, the electroosmotic flow is suppressed in an acidic medium because at this pH, the silica capillary surface bears no negative charge. Thus, the transport consists only of the electrophoretic part. In addition to electric force, hydrodynamic force also affects analytes mobility. This force comes from the different type of "frictions" of the medium or viscosity, and also from the relaxation effect of the counter ion cloud.

Although the charge/mass ratio values of dendrimers are almost constant, it was found that the mobility of PAMAM dendrimers decreases with increasing generation number. This can be explained by the decrease in the charge/surface area ratio with increasing number of generation. The actual surface areas increase with the increase in generations as reported by Maiti et al. [39]. Another possible explanation is that anions (such as H_2PO_4 ions) may partially shield the charge or "neutralize" the protonated amine groups, thereby decreasing charge to surface area ratios and thus, lowering mobility.

It is also known that amine-terminated PAMAM dendrimers (which carry positive charge at low pH) have a strong tendency to be adsorbed onto negatively charged silica or glass surfaces [40-42]. As a consequence, separations are often irreproducible, even when the same sample, instrument, capillary and run conditions were employed. In order to decrease the adsorption of protonated PAMAM dendrimers on the silica substrate, a silanization reaction was performed by derivatizing the surface silanol groups of the capillary with chlorotrimethylsilane. This increased reproducibility due to the increase hydrophobic methyl groups on the capillary surface [17].

Fig 3.4 shows is an electropherogram showing the separation of PAMAM dendrimers on a silanized capillary. As expected, this approach shows a rapid decrease in migration time, almost cutting it in half (migration time for generation

2 was ~12 minutes in a silanized capillary compared to ~22 minutes using a bare fused silica capillary in fig 3.3).

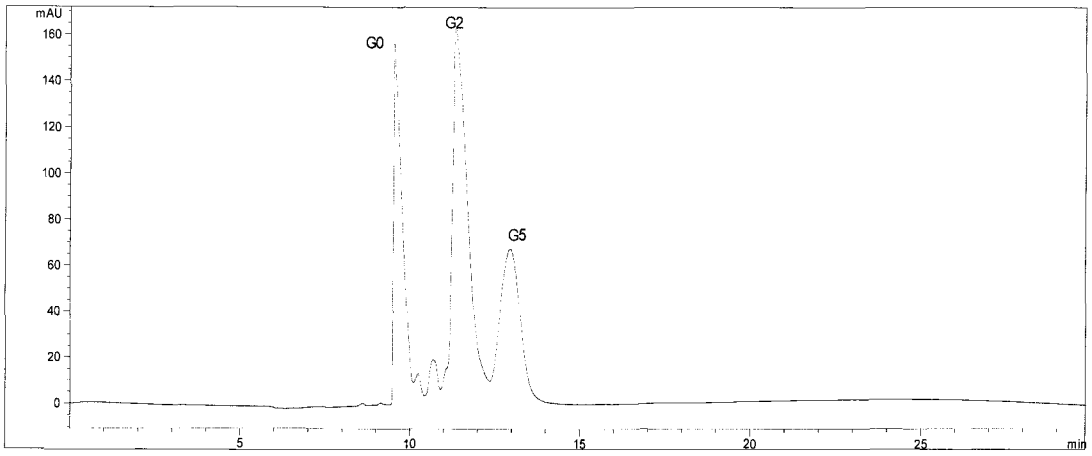

Figure 3.4 CZE separation of generation 0, 2, and 5 Starburst dendrimers using silanized capillary
Conditions: capillary column, 75 μm ID x 360 μm OD x 50 cm (effective length); 20 kV applied voltage; UV detection at 200 nm; mobile phase, 0.05M phosphate buffer pH 2.7.

An interesting note is that silanization seems to decrease the adsorption on silica wall over time, but does not eliminate it. As subsequent runs were repeated, the migration times slowly decreased until finally they stabilized at a steady value. Fig 3.5 shows the plot of migration times of dendrimers in their consecutive runs using a silanized capillary. As opposed to the long migration times (20–25 min) of the first two runs reported by Shi et al. [17] and decreasing rapidly in the consecutive runs approaching a plateau, our runs showed a migration times of 12-16 minutes for the first 2 runs, rapidly stabilizing to 9-13 minutes. This might be caused by the difference in degree of effectiveness of the silanization reaction, i.e. how efficiently the silanol groups were derivatized, which may be affected by the

amount of reagent or for how long. The conditioning and equilibriation steps between each run were also important to achieve higher reproducibility. The RSD of migration times of dendrimer samples on the same day was calculated and found to be less than 4.0% (see Table 3.3). Day-to day reproducibility, however, was low. Thus, day-to-day measurements still needed improvement.

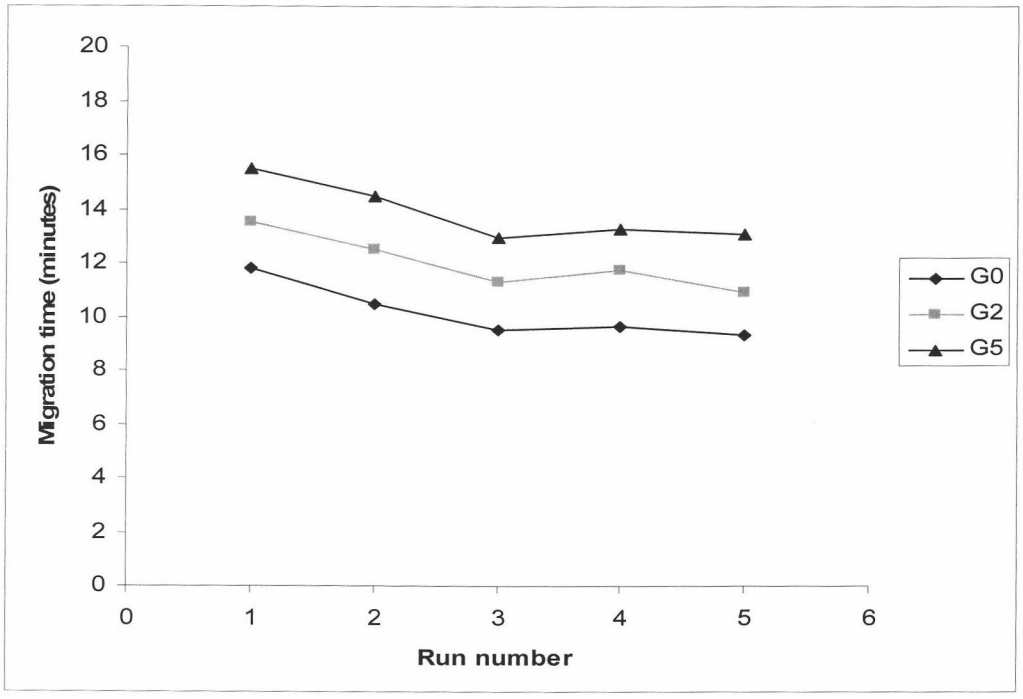

Fig 3.5 Relationship between the migration time and consecutive run numbers for generation 0,2,5 PAMAM dendrimers on silanized capillary. For run conditions, see fig 3.4.

PAMAM dendrimers	G0	G2	G5
Migration time t_m (min)	9.90	11.7	13.4
RSD of t_m	3.99%	3.12%	2.06%
Electrophoretic mobility ($cm^2/V.s$)	0.000596	0.000504	0.000443

Table 3.3 Migration times of PAMAM dendrimers and their RSD analyzed using a silanized silica capillaries. The migration time is the average of three measurements using the same capillary and same CE conditions on the same day.

Peak shapes were also compared between runs done using bare fused-silica and silanized capillaries. Non-Gaussian peak shapes were usually observed for the first runs, particularly using the bare fused silica capillaries. On the other hand, Gaussian peak shape is prominent on electropherograms recorded after several runs, particularly for the higher generation dendrimers. This indicates strongly non-linear adsorption, and generation 5 dendrimer is preferably retained from the mixture, which is indicated by the much smaller area under the peak.

The electrophoretic mobility μ_0 for PAMAM dendrimers was also calculated using equation 3.2 below [43] where EOF is negligible at pH 2.5.

$$\mu_0 = (lL/Vt_m) \qquad (3.2)$$

where l is the effective length of the capillary (from inlet to detector window), L is the total length of the capillary (both in cm), V is the applied voltage, and t_m is the migration time (min). The electrophoretic mobility for generation 0, 2, and 5 PAMAM dendrimers were recorded in table 3.3.

Besides for generational separations, CZE can also be used for analyzing structural errors in low generation dendrimers since there are numerous possible side reactions present in the mixtures. There are at least three types of structural errors in PAMAM dendrimer synthesis: (1) missing arms, which resulted from incomplete Michael addition during the divergent method causing the appearance of asymmetrice dendrimeric structures (Fig. 3.6 A), (2) in order to suppress the

formation of missing arms, excess of EDA is used, but it may lead to the formation of dimers (or oligomers) (Fig 3.6 B), and (3) intramolecular cyclization, which results during the formation of a full-generation dendrimer when many functional groups are present in the outer shell. And therefore, different cyclization possibilities can result (Fig. 3.6 C).

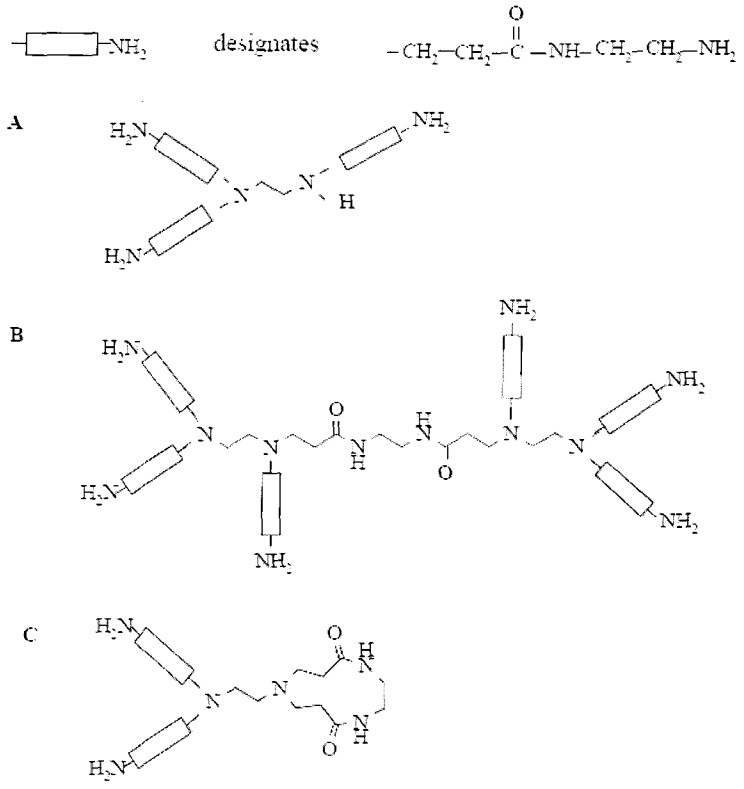

Fig 3.6 Defective structures of generation 0 PAMAM dendrimer: (A) missing arm, (B) dimer, and (C) intramolecular cyclization [16]

Figure 3.7 shows a CZE electropherogram of single generation (generation 0) synthesized by our research group, which allows the assessment of the presence of side products in synthesized dendrimers. From the figure, the electropherogram consists of the peak for the target generation, along with peaks for the previous generation and side products or impurities attributed to the structural errors. The impurities that are migrating slower than the main component may be attributed to intermolecular cyclization (fig 3.6 C). At each cyclization, the molecule loses 60 Da of mass and two terminal amino groups, and therefore possess an increased mass-to-charge ratio, and thus lower electrophoretic mobilities.

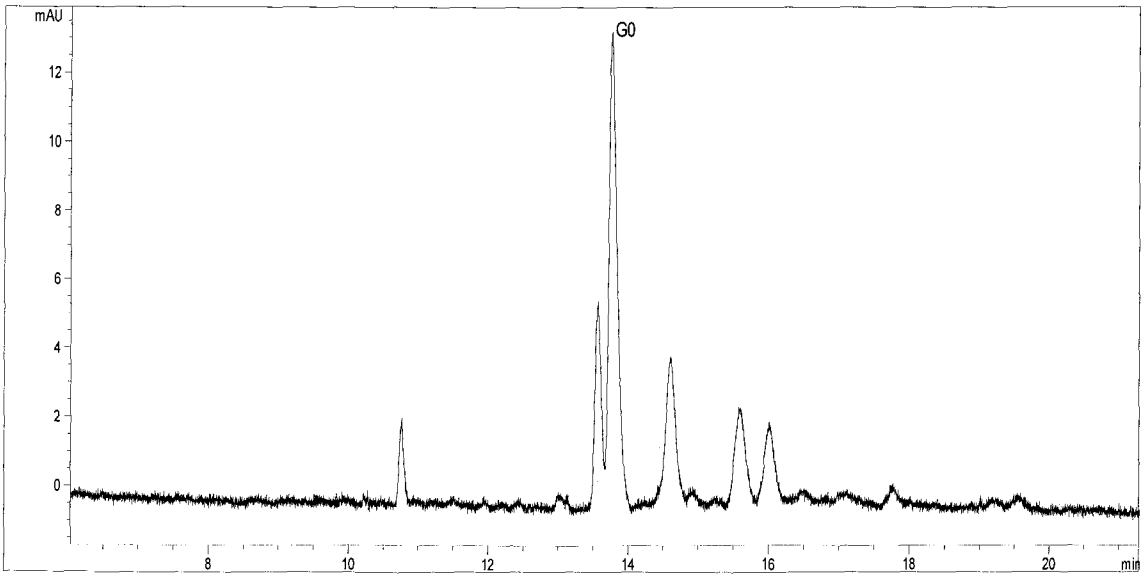

Fig. 3.7 Electropherogram of synthesized dendrimer generation 0 from several side products. Conditions: capillary column, 75 μm ID x 360 μm OD x 50 cm (effective length); 20 kV applied voltage; UV detection at 200 nm; mobile phase, 0.1M phosphate buffer pH 2.7

3.3.1.2 Capillary Electrophoresis of Carboxyl-terminated PAMAM dendrimers

In contrast to full-generation dendrimers, half-generation PAMAM dendrimers possess carboxyl groups on the surface (fig. 1.3). Therefore, they are not ionized at low pH values, and separations performed under this pH were not successful. Rather, the use of higher pH (pH~8) allows half-generation dendrimers to have multiple negative charges since at this pH, tertiary amines (pKa 4-5) are not protonated [1, 36], while the terminal carboxyl groups are deprotonated.

Therefore, in the case of half-generation dendrimers, the electrophoretic mobility of the carboxylate anions is against the EOF. Under the applied electric field, they migrate towards the anode while the cathode directed EOF migrates faster than the anions.

The use of basic solution in the case of half-generations dendrimers, however, becomes problematic in trying to separate a mixture of half-generations dendrimers since they are markedly labile and hydrolyze readily in buffer solution. Fig 3.8 shows the CE electropherogram of carboxyl-terminated PAMAM dendrimers exhibit multiple peaks derived from hydrolysis of PAMAM half-generation esters [21].

From fig 3.8, it was apparent that when the samples stayed in buffer for hours, hydrolysis occurred. Hydrolysis of half-generation PAMAM dendrimers occurred during the intermediate steps, i.e. from amidic intermediate to carboxylate terminal groups (fig 1.3). This can be an advantage for observing

various carboxylate anions and kinetics of hydrolysis. However, for our purpose, separations of a mixture of half-generation dendrimers could not be performed by CZE, so other methods were developed.

(a)

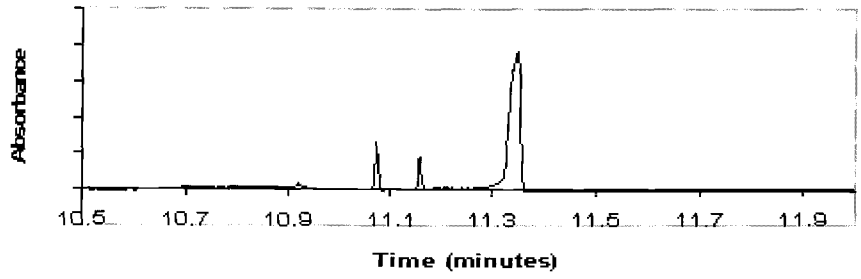

(b)

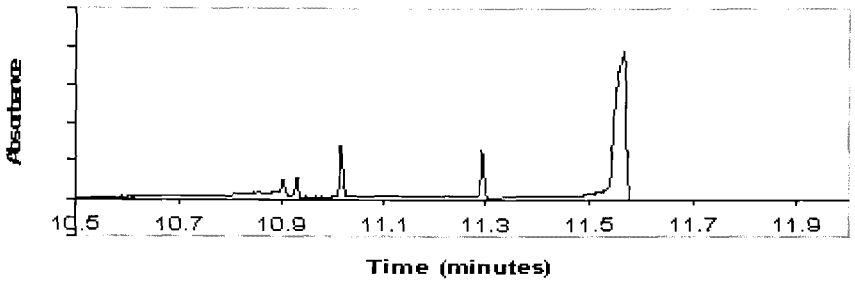

(c)

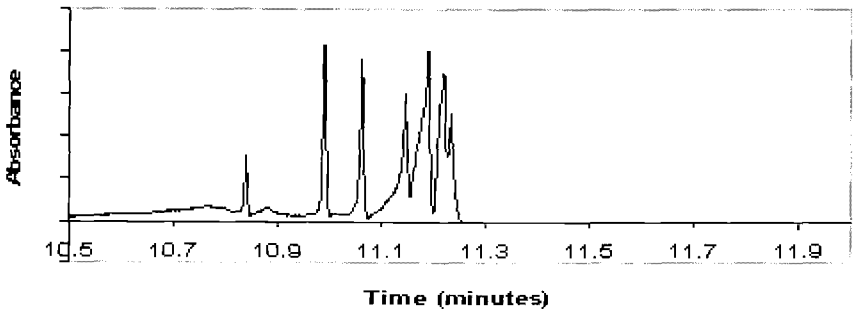

Fig 3.8 Electropherogram of PAMAM dendrimer generation 4.5 (a) run immediately after dissolving in buffer solution, (b) run ~2 hours after dissolving, (c) run ~3.5 hours after dissolving in buffer solution.

3.3.2 Capillary electrochromatography (CEC)

Monolithic polymer sorbents were prepared for CEC using PAMAM dendrimers as template molecules to produce uniform pore structures and to influence the surface chemistry of the finished polymer. A preliminary result from our research group has shown that different pore size can be obtained by simply optimizing the dendrimer template concentration. The column efficiency and resolution increased when the sorbent was templated with PAMAM dendrimer, as opposed to using a monolithic column with no template [34].

Figure 3.9 shows the SEM image of a monolithic column prepared using 150 uM dendrimers; demonstrating that a highly permeable monolith was achieved, which is essential for their application as sorbents in chromatographic separations. From fig 3.9 a) and b), it is apparent that aggregates of micrometer-sized globular particles were extended throughout the capillary. These aggregates were surrounded by 1-20μm wide pores, which permitted bulk flow throughout the capillary. In fig 3.9c), covalent attachment of the polymer to the capillary wall can be seen. These attachments were very stable that even hydrodynamic pressures up to at least 1000 psi were permitted without polymers eluting out of the capillary.

A)

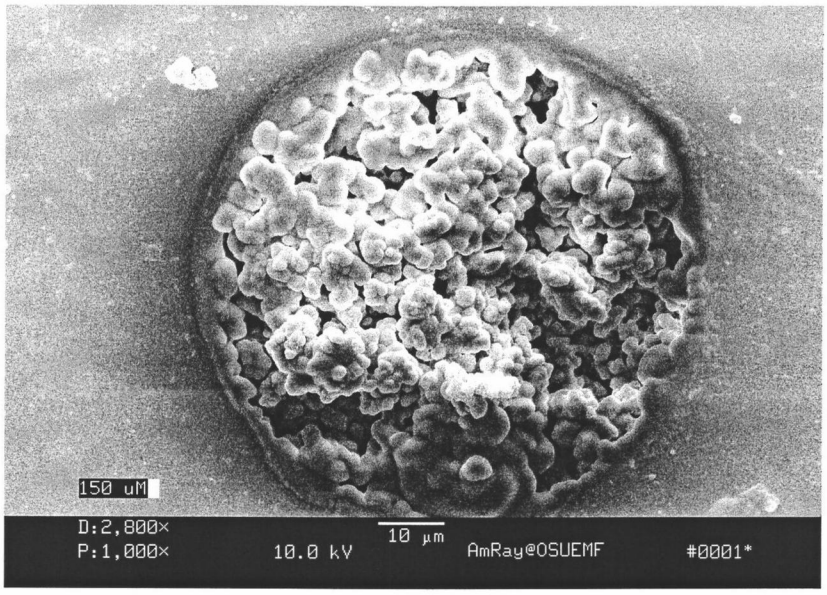

B)

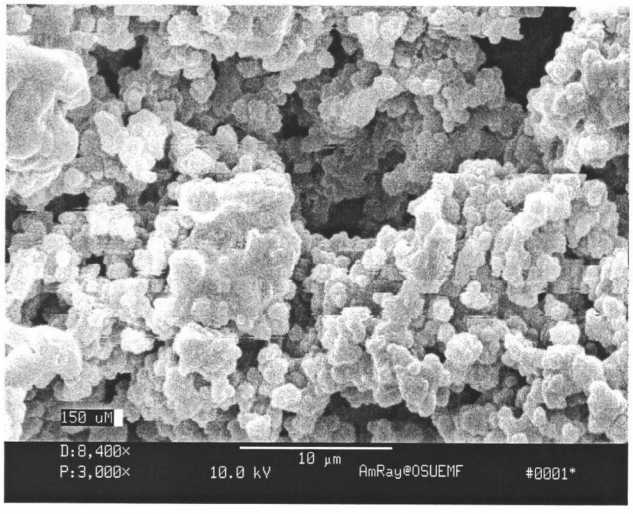

C)

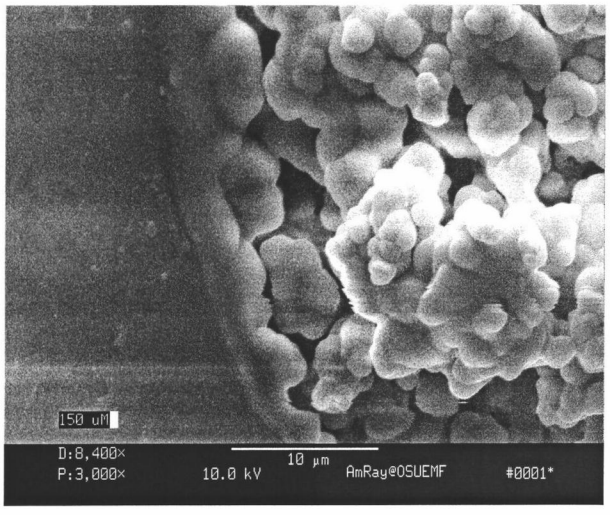

Fig. 3.9 (a) Scanning electron micrograph (SEM) image of a monolithic column with 200 µM dendrimer template, (b) Close view of the monolithic bed (magnified from (a)), (c) The covalent attachments of the polymer to the capillary wall can be seen.

Our first attempt was to prepare a monolithic column templated with 200 uM dendrimer generation 2.5. The column was prepared using butyl methacrylate (BMA) as a hydrophobic monomer. In this case, the stationary phase resembles RP-HPLC to affect separation. In addition, the stationary phase in CEC also has a role in generating EOF, thus an addition of charged (hydrophilic) functionalities is necessary. As mentioned before, the template itself (dendrimer) has a dual role: 1) to control pore structures, 2) to influence the surface chemistry of the finished polymer. Fig 3.10 shows the separation of generation 0.5 PAMAM using dendrimer-templated monolithic column.

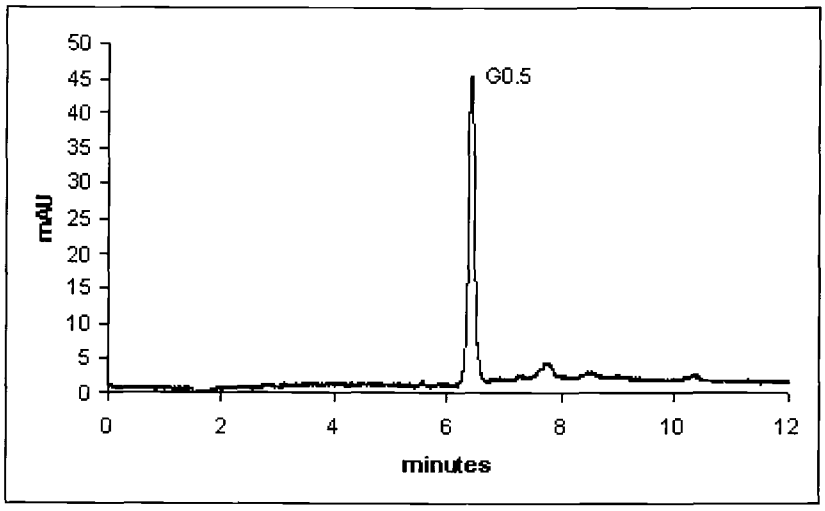

Fig. 3.10. Electropherogram of generation 0.5 Starburst dendrimers using generation 2.5 dendrimer-templated monolithic sorbent. Conditions: capillary column, 75 μm ID x 360 μm OD x 25 cm (effective length); 20 kV applied voltage; pressure in vials, 0.2 MPa; injection 5 kV for 5 s; UV detection at 200 nm; mobile phase, 0.1M phosphate buffer pH 7.8.

As can be seen from the figure, the migration time is about 6 minutes. Compared to a bare-fused silica capillary, separations using monolithic columns are more reproducible when injecting fresh sample each time (t_m RSD = 5.96% for n=4). As expected, the efficiency increases from 8020 plates/m (without dendrimer template) to 61620 plates/m using dendrimer-templated monolithic column.

Another sorbent was also prepared with the same polymerization mixture, differing only in the amount and type of template molecule. In this case, dendrimer generation 5 was used as template molecule. The migration time of generation 5 dendrimer was about 6 minutes (electrophoretic mobility of 1.69×10^{-4} $cm^2/V.s$), decreasing greatly compared to bare-fused silica capillaries (almost 30 minutes). This is in part is attributed to the increase in hydrophobicity of the stationary phase, compared to bare-fused silica capillaries in CZE, and thereby adsorption to the stationary phase is reduced in acidic medium, and separations are more reproducible. Unfortunately, separations of generations 2, 4 and 5 using this sorbent resulted in peaks that were unresolved.

This limitation has led to the need to obtain higher selectivity, particularly for higher generation dendrimers as generational separation of dendrimers with high molecular masses still poses problems. Subsequently, generation of selective sorbents in the form of templated polymers with surfaces containing sites that are complementary in shape and chemical functionality to the dendrimer template molecule were followed.

Here, the template structure must contain chemical functional groups capable of interacting with the monomer(s) with sufficient strength to form a stable complex through mainly hydrogen bonding or electrostatic interactions. A column where all MAA monomer was replaced with BMA was not able to differentiate between different dendrimer generations, which indicated the necessity of MAA that allows hydrogen bonding interactions with the analyte. The template molecule was generation 5 PAMAM dendrimer, and our first trial incorporated MAA as the functional monomer, which can also provide EOF in CEC.

Since it has been reported that replacing a part of the functional monomer MAA by other weaker interacting monomers (methyl, butyl, or epoxypropyl methacrylate) could to a certain extent improve template recognition, and thus improve the efficiency and resolution [45], monolithic columns with BMA and MAA as the monomers were prepared (table 3.4).

Figures 3.11 and 3.12 show separations of generations 2, 4, and 5 using dendrimer templated monolithic columns with varying monomer concentrations (table 3.4). As can be seen from fig. 3.11, the templated molecule (G5) was preferentially retained in the column (monolithic column B), which is indicated by the much smaller area under the peak ($t_R \sim 28$ minutes). Changing the monomer concentration (monolithic column C) resulted in G5 dendrimer heavily retained in the column (fig. 3.12). Flushing with high pH solution at high pressure and voltage eluted the peak for template molecule out the column. Thus, high selectivity for the template was then achieved using the sorbent.

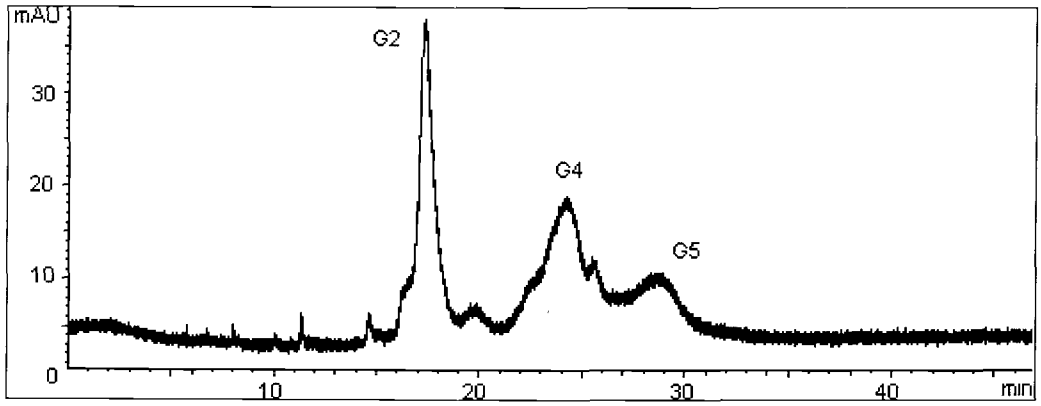

Fig. 3.11 Electropherogram of generation 2, 4, and 5 Starburst dendrimers using G5 dendrimer-templated monolithic sorbent (monolithic column B). Conditions: capillary column, 75 μm ID x 360 μm OD x 25 cm (effective length); 20 kV applied voltage; pressure in vials, 0.2 MPa; injection 5 kV for 5 s; UV detection at 200 nm; mobile phase, 0.1M phosphate buffer pH 2.7.

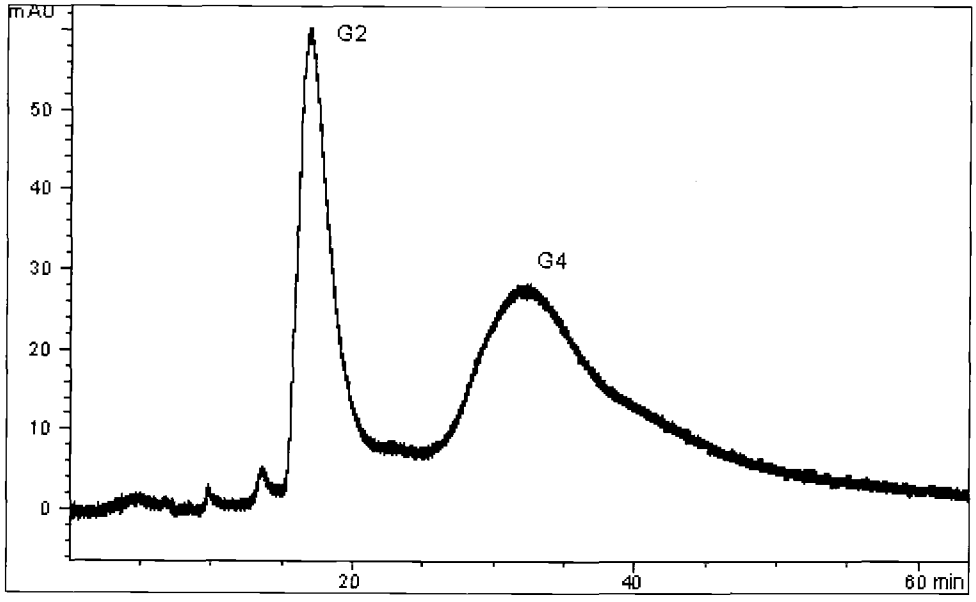

Fig. 3.12 Electropherogram of generation 2 and 4 Starburst dendrimers using G5 dendrimer-templated monolithic sorbent (monolithic column C). G5 dendrimer was retained in the column. The peak could be observed after applying high pressure and voltage. For conditions, see fig 3.11.

Monolithic column	Monomer (BMA:total monomer)[a)]	Template (μM)	Analyte	Efficiency (plates/m)	t_R (min)	Selectivity
B	37.5%	200 μM	G2	12908	17.317	
		G5	G4	5804	24.218	1.40
			G5	2404	28.838	1.19
C	25%	200 μM	G2	2583	16.869	
		G5	G4	533	31.930	1.89

Table 3.4 CEC evaluation of dendrimer separation using templated monolithic columns
[a)]Calculated from the mol amounts in the polymerization mixture according to [BMA/(BMA+MAA+EGDMA)]x100

The effect of incorporation of BMA was an increase in separation capability in terms of efficiency for both non-imprinted and imprinted analytes. As can be seen in table 3.4, the efficiency is higher in monolithic column containing more BMA monomer (12908, 5804, and 2404 plates/m for generation 2, 4, and 5, respectively). The selectivity, however, is higher in the MAA-containing monolithic column, even though it yielded stronger retention and lower efficiency. This could be due to the slow association/dissociation kinetics of the analyte with the polymer, which is a common problem in MAA-based templated columns. This monomer is more hydrophilic than BMA and the longer retention time indicates a hydrophilic interaction component in the retention mechanism.

Since the MAA-containing sorbent gave the higher selectivity, but the efficiency was superior in BMA-containing sorbent, a complex mechanism needs to be considered regarding improved polymer characteristic, and thus separation performance. I hypothesize that there is a complex formed between the template and the functional monomer in the pre-polymerization mixture, leading to better

defined imprints and/or effects regarding the adsorption and desorption kinectics of interactions during CEC.

3.3.3 High Performance Liquid Chromatography (HPLC)

Separations in reverse phase (RP)-HPLC are based on partitioning of analytes between the hydrophobic surface of stationary phase and the eluent. Unlike CE, neutral as well as anionic and cationic compounds can all be separated in HPLC. In this case, HPLC is suitable for separating analytes with different surface functionalities. Separations between full- and half-generation dendrimers, which were not possible using CE, were therefore explored with HPLC.

Fig 3.13 shows the chromatogram of various generations of amine-terminated dendrimers. The assignment of peaks was based on single runs of each dendrimer. Blank injection was also made by injecting fresh solvent under the same run conditions. As can be seen from the figure, the hydrophobicity of amine-terminated PAMAM dendrimers decreases as a function of generation. Thus, lower generation dendrimers are retained longer and elute last, when separated by RP-HPLC.

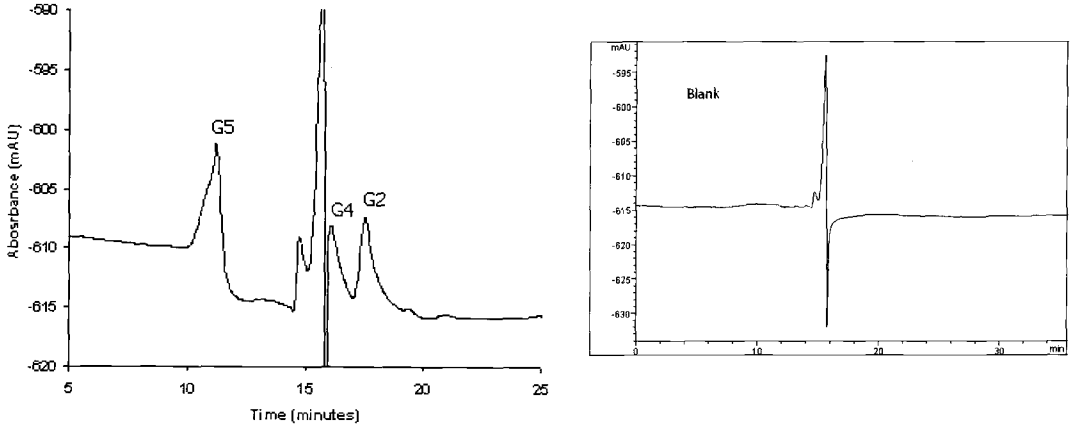

Fig. 3.13 A mixture of 1 mg/ml full generation 2, 4, and 5 PAMAM dendrimers at 200 nm. Column: Beckman Ultrasphere C-8, 5μm, 4.6mm x 25 cm. Chromatographic conditions: Flow rate: 0.2 ml/min, mobile phase: 80:20 H_2O/ACN

As it is well known that amine-terminated PAMAM dendrimers adsorb to strongly the surface of silica support particles of the column, trifluoroacetic acid (TFA) was added to the mobile phase (ACN/H_2O) at a concentration of 0.1 wt %, which resulted in a pH of 2 in the aqueous phase [26] to attenuate the problem. At this acidic pH, both primary and tertiary amines are protonated [46]. Thus, the addition of counterion TFA will create PAMAM-TFA complexes through ionic interactions, which then partitioned on the RP-HPLC columns. As expected, the adsorption to the sorbent is minimized and the peak shape is improved (fig. 3.14).

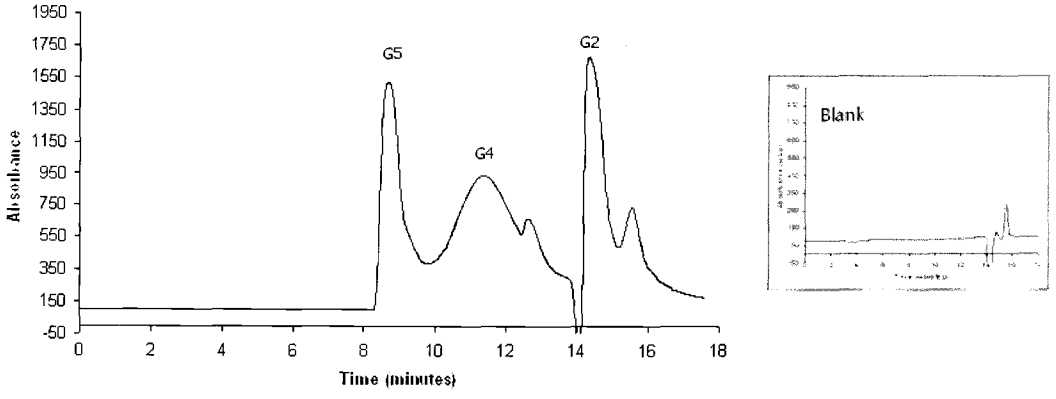

Fig. 3.14 A chromatogram of a mixture of 1 mg/mL full-generation 2, 4, and 5 Starburst dendrimers
Conditions: column, Beckman Ultrasphere C-8, 250 x 4.6mm, 5μm particle size; mobile phase: 80:20 v/v mixture of H_2O:acetonitrile (0.1 wt % TFA each); flow rate, 0.2 mL/min; UV detection at 200 nm.

In addition to separating various amine-terminated PAMAM dendrimers, the potential use of HPLC to separate full and half generation dendrimers was explored. Fig 3.15 shows the chromatogram of a mixture of amine and carboxyl-terminated PAMAM dendrimers. Hydrophobicity increases as the surface changes from amine to carboxyl groups, such that half generation dendrimers are retained longer and eluted last. The addition of TFA, in this case to lessen the adsorption of the dendrimer to the column, affects only the amine-terminated dendrimer (as at acidic pH the amine group is protonated, but not the carboxyl group).

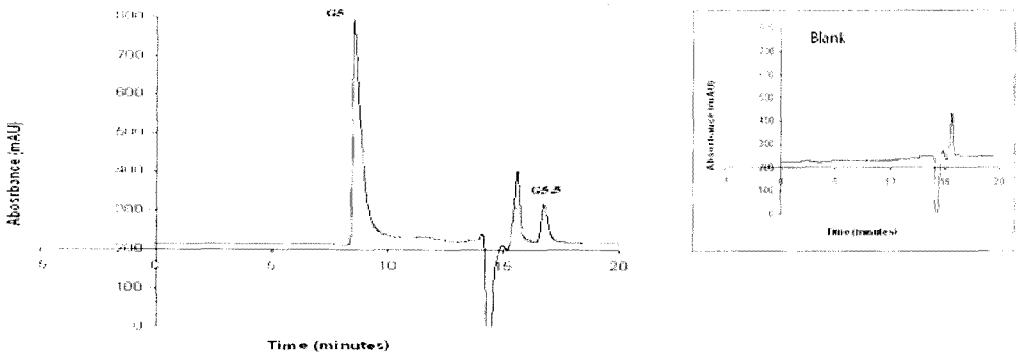

Fig. 3.15 A chromatogram of a mixture of 1mg/mL generation 5 and 5.5 Starburst dendrimers.
Conditions: column, Beckman Ultrasphere C-8, 250 x 4.6mm, 5µm particle size; mobile phase: 80:20 v/v mixture of H_2O:acetonitrile (each contains 0.1 wt. %TFA); flow rate, 0.2 mL/min; UV detection at 200 nm.

3.4 Conclusions

Separations of various generations of PAMAM dendrimers were analyzed using CZE, CEC, and HPLC. CZE provides efficient separations of various full-generation dendrimers. Generational separations up to the fifth generation were achieved in acidic (pH 2.7) conditions. However, a complex separation mechanism is found for full-generation PAMAM dendrimers. Although an electrical potential gradient moves PAMAM dendrimers into the capillary (based on their effective charge/surface area ratios), the CE separation was based on differences in adsorption/desorption of dendrimers on the capillary surface - not the desired mechanism in CE. An electropherogram of a single generation product, though, is a valuable tool that allows for assessing the homogeneity and presence of side products in synthesized dendrimers.

A simple and quick method for the in situ preparation of monolithic columns for CEC with dendrimer-templated porosity was demonstrated. This approach delivered sorbents with more controlled porosity and higher selectivity than the current CE methods [16, 17]. Separations of dendrimers of various generations were achieved using these sorbents.

Finally, findings from these studies indicate that HPLC can be used to separate dendrimers of various generations. Full-generation separations up to generation 5 were achieved using an RP-HPLC method. Separations of dendrimers with terminal amino and carboxyl groups were obtained using the same method.

References

[1] Tomalia, D. A., Baker, H., Dewald, J. A., Hall, M., Kallos, G., Martin, S., Roeck, J., Ryder, J., Smith, P., *Macromolecules* **1986**, *19*, 2466.

[2] Tomalia, D. A., Baker, H., Dewald, J. R., Hall, M., Kallos, G., Martin, S., Roeck, J., Ryder, J., Smith, P., *Polym. J.* **1985**, *17*, 117.

[3] Wiener, E.C., Auteri, F.P., Chen, J.W., Brechbiel, M.W., Gansow, O.A., Schneider, D.S., Belford, R.L., Clarkson, R.B. & Lauterbur, P.C. *J. Am. Chem. Soc.* **1996**, *118*, 7774–7782.

[4] Bryant, L.H., Brechbiel, M.W., Wu, C., Bulte, J.W.M., Herynek, V. & Frank, J.A. *J. Magn. Reson. Imaging* **1999**, *9*, 348–352.

[5] Bourne, M.W., Margerun, L., Hylton, N., Campion, B., Lai, J.J., Derugin, N. & Higgins, C.B. *J. Magn. Reson. Imaging*. **1996**, *6*, 305–310.

[6] Fischer, M. & Vögtle, F. *Angew. Chem., Int. Edn.* **1999**, *38*, 884–905.

[7] Twyman, L.J., Beezer, A.E., Esfand, R., Hardy, M.J. & Mitchell, J.C. *Tetrahedron Lett.* **1999**, *40*, 1743–1746.

[8] Liu, M., Kono, K. & Fréchet, J.M.J. *J. Controlled Release 65*, 121–131.

[9] Zhuo, R.X., Du, B. & Lu, Z.R. *J. Controlled Release* **2000**, *57*, 249–257.

[10] Hawthorne, M.F. *Angew. Chem., Int. Edn.* **1993**, *32*, 950–984.

[11] Barth, R.F., Adams, D.M., Soloway, A.H., Alam, F. & Darby, M.V. *Bioconjug. Chem.* **1994**, *5*, 58–66.

[12] Liu, L., Barth, R.F., Adams, D.M., Soloway, A.H. & Reisefeld, R.A. *J. Hematotherapy*. **1995**, *4*, 477–483.

[13] Capala, J., Barth, R.F., Bendayam, M., Lauzon, M., Adams, D.M., Soloway, A.H., Fenstermaker, R.A. & Carlsson, J. *Bioconjug. Chem.* **1996**, *7*, 7–15.

[14] Bielinska, A.U., Kukowska-Latallo, J.F., Johnson, J., Tomalia, D.A. & Baker, J.R. *Nucleic Acids Res.* **1996**, *24*, 2176–2182.

[15] Kukowska-Latallo, J.F., Raczka, E., Quintana, A., Chen, C.L., Rymaszewski, M. & Baker, J.R. *Hum. Gene Therapy* **2000**, *11*, 1385–1395.

[16] Ebber, A., Vaher, M., Peterson, J., Lopp, M. *J. Chromatogr. A* **2002**, *949*, 351-358

[17] Shi, X., Ba´nyai, I., Lesniak, W., Islam, M. T., Orsza´gh, I., Balogh, P., Baker, J. R., Jr., Balogh, L. *Electrophoresis*, **2005**, *26*, 2949-2959

[18] Shi, X., Patri, A. K., Lesniak, W., Islam, M. T., Zhang, C., Baker, J. R., Jr., Balogh, L. *Electrophoresis*, **2005**, *26*, 2960-2967

[19] Majoros, I. J., Keszler, B., Woehler, S., Bull, T., Baker, J. R., Jr. *Macromolecules* **2003**, *36*, 5526-5529.

[20] Tan, N. C. B., Balogh, L., Trevino, S. F., Tomalia, D. A., Lin, J. S. *Polymer* **1999**, *40*, 2537-2545.

[21] Brothers II, H. M., Piehler, L. T., Tomalia, D. A., *J. Chromatogr. A* **1998**, *814*, 233–246.

[22] Balogh, L., Leuze-Jallouli, A., Dvornic, P., Kunugi, Y., Blumstein, A., Tomalia, D. A., *Macromolecules* **1999**, *32*, 1036–1042.

[23] Tomalia, D. A., Huang, B., Swanson, D. R., Brothers, H. M., Klimash, J.W., *Tetrahedron* **2003**, *59*, 3799–3813.

[24] Huang, Q. R., Dubin, P. L., Moorefield, C. N., Newkome, G. R., *J. Phys. Chem.* **2000**, *104*, 898–904.

[25] Choi, Y., Thomas, T., Kotlyar, A., Islam, M. T., Baker, J. R., Jr. *Chem. Biol.* **2005**, *12*, 35-43.

[26] Islam, M. T., Shi, X., Balogh, L., Baker, J. R., Jr. *Anal. Chem.* **2005**, *77* (7), 2063-2070.

[27] Islam, M. T., Majoros, I. J., Baker, J. R., Jr. *J. Chromatogr., B: Anal. Technol. Biomed. Life Sci.*, **2005**, *822,* 21-26

[28] Schwartz, B. L., Rockwood, A. L., Smith, R. D., Tomalia, D. A., Spindler, R. *Rapid Commun. Mass Spectrom.* **1995**, *9*, 1552-1555.

[29] Kallos, G. J., Lewis, S., Zhou, J., Hedstrand, D. M.; Tomalia, D. A. *Rapid Commun. Mass. Spectrom.* **1991**, *5*, 383.

[30] Woller, E. K., Cloninger, M. J. *Biomacromolecules* **2001**, *2*, 1052- 1054.

[31] Mitnik, L., Novotny, M., Felten, C. *Electrophoresis* **2001**, *22*, 4104-4117.

[32] Patrick, J. S., Lagu, A. L. *Electrophoresis* **2001**, *22*, 4179-4196.

[33] Righetti, P. G. *Biopharm. Drug Dispos.* **2001**, *22*, 337-351.

[34] Doneanu, A., Chirica, G., Remcho, V.T. *Journal of Separation Science.* **2002**, *25*, 1252-1256

[35]Hjerten, S. *J. Chromatogr.* **1985**, *347*, 191-195

[36] Tomalia, D. A., Naylor, A. M., Goddard, W. A., III. *Angew. Chem., Int. Ed. Engl.* **1990**, *29*, 138.

[37] Cakara, D., Kleimann, J., Borkovec, M., *Macromolecules* **2003**, *36*, 4201–4207.

[38]Shi, C, Majoros, I, Baker, J.R. *Molecular Pharmaceutics*. **2005**, *2*, 278-294

[39]Maiti, P. K, Cagin, T, Wang, G, Goddard, W. *Macromolecules*, **2004**, *37*, 6236-6254

[40] Esumi, K., Goino, M.. *Langmuir* **1998**, *14*, 4466-4470.

[41] Ottaviani, M. F., Turro, N. J., Jockusch, S., Tomalia, D. A.. *J. Phys. Chem. B* **2003**, *107*, 2046-2053.

[42] Tsukruk, V. V., Rinderspacher, F., Bliznyuk, V. N.. *Langmuir* **1997**,*13*, 2171-2176.

[43] Li, S. F. Y., *Capillary Electrophoresis Theory & Practice.* Academic Press, San Diego, CA **1992**.

[44] Rahman, K. M. A., Durning, C. J., Turro, N. J., Tomalia, D. *Langmuir* **2000**, *16*, 10154-10160.

[45] Schweitz, L, Andersson, L, Nilsson, S. *Analyst* **2002**, *127*, 22-28

[46]Mengerink, Y, Mure, M, de Brabander, E.M.M, van der Wal, Sj. *J. Chromatogr.*, A **1996**, *730*, 75

[47] Pesak, D. J., Moore, J. S., Wheat, T. E., *Macromolecules* **1997**, *30*, 6467–6482.

[48]Castagnola, M., Zuppi, C., Rossetti, D. V., Vincenzoni, F., Lupi, A., Vitali, A., Meucci, E., Messana, I., *Electrophoresis* **2002**, *23*, 1769–1778.

[49] Jung, H. J., Bae, Y. C., *J. Polym. Sci. Polym. Chem.* **2002**, *40*, 1405–1420.

[50] Bruggemann, O., Freitag, R., Whitcombe, M. J., Vulfson, E. N., *J. Chromatogr. A* **1997**, *781*, 43–53.

CHAPTER 4

MICROFLUIDIC CHIPS FOR DENDRIMER ANALYSIS

Abstract

The present chapter focuses on the CE-based separation of PAMAM dendrimers on a microchip. Microfluidic devices offer unique advantages in sample handling, reagent mixing, separation, and detection. Separation conditions have been optimized for the electrophoretic separations of TAMRA-labeled dendrimers in glass microfluidic channels with laser-induced fluorescence detection. The method used for the analysis was transferred from the on-column CE method into the glass microchips. Generation 0 and 2 PAMAM dendrimers were successfully detected in 50 mM phosphate buffer pH 2.7 with a retention time of about 60 seconds.

4.1. Introduction

Significant progress has been made in the development of microfluidic devices since the initial concept was introduced 15 years ago [1]. Microfluidic devices are often described as miniature versions of their macro-scale counterparts. Since the introduction of the first commercial microfluidic lab-on-a-chip based systems for life science applications, the field has grown immensely as can be seen from the growing numbers of microfluidics companies, microfluidic-based

products, and publications in the last few years. In fact, trends suggest that microfluidics will be the next big step in the development of chemical analysis [2].

Microfluidic chips offer unique advantages that have attracted considerable attention. Compared to their larger-scale conventional counterparts, microfluidic devices offer smaller sample and reagent volumes. Expensive and difficult-to-obtain samples and reagents are thus accessible in routine analysis, since only nano- to microliter quantities of samples and reagents are required. In addition, the use of small volumes of samples and reagents will produce less waste and harmful byproducts. Microfluidic channel dimensions, typically are in the 10-100 micrometer range in both width and height and only 1-5 cm in length, thus analysis times are often decreased. The use of short channels has also made possible the development of portable analytical instrumentation where lower voltages and smaller power supplies are required and achievable, leading to practical portable analysis systems. Microfluidic devices are also amenable to inclusion in highly integrated parallel systems, where multiple individual analytical operations can be performed and automated. Plastic microfluidic devices can be made disposable due to the very low cost of producing them. Finally, their ability to handle all steps of the analysis on one chip, from sampling, sample processing, separation and detection steps to waste handling, allows for the development of micro total analysis systems (Micro-TAS). This integration makes complex analyses simpler to perform.

Since the introduction of the micro-total analysis systems, microchip capillary electrophoresis (CE) has been investigated as an attractive separation

technique. Microchip CE has been applied to a wide range of applications, including environmental monitoring, biomedical and pharmaceutical analysis, clinical diagnostics, and forensic investigations [3-6]. Numerous reports have been published regarding the successful transition of CE systems to the microchip platform [7-10]. As there is no fundamental operational difference between microchip CE and conventional CE systems, the theory developed for capillaries is readily applicable to channels in microchips. Typical microchip channel sizes are 10-100 μm in width and depth, similar to the dimensions of fused silica capillaries as used in conventional CE.

The same separation mechanism applies in microfluidic devices as in conventional CE. When an electric potential is applied parallel to the channel walls, charged species will separate based on differences in their electrophoretic mobilities. Electroosmotic flow (EOF) is the bulk driving force, which is dependent on the interaction between the channel wall surfaces and the enclosed fluid. Since the fluid flow is driven by EOF, the device does not include mechanical pumps or valves, such that backpressure effects are minimized. In addition, the flat flow profile generated by EOF minimizes dispersion of analyte, allowing very high efficiency.

Glass has been the most widely used substrate for CE microchips [11-12] owing to many benefits. As mentioned before, the chemistries developed for fused-silica capillaries are similar to those for glass, allowing for direct transfer from one format to another. Glass is resistant to many chemicals, can withstand high voltages that are employed in electrokinetically driven separations, and

possesses high thermal stability and biocompatibility. Moreover, these substrates are optically transparent and allow detection of the analytes by laser-induced fluorescence and other optical methods. The microfabrication process in glass is well-understood and easily implemented. Despite their advantages, glass chips also have some limitations, namely their high unit cost and harmful fabrication procedure. Glass is relatively expensive and fragile and can often break during microchip fabrication. A well-equipped cleanroom is required, and the use of hydrofluoric acid (HF) for substrate etching requires special safety precautions. Nevertheless, glass microchips continue to be employed successfully for the separation of many analytes. The use of polymers [13-16] as alternative materials for microchips that exhibit similar properties to glass, but are cheaper and easier to fabricate, is still investigated.

Fabrication of microfluidic devices mostly follows lithographic procedures that have been used for many years by the electronics industry. Glass CE microchips are fabricated using standard photolithographic techniques [17-18] as depicted in fig. 4.1. First, a thin layer of metal is deposited into the entire surface of a substrate, which is used as a protective layer to promote adhesion of photoresist to the substrate during the etching process. Photoresist is then spin-coated onto the substrate and is exposed to UV radiation through a mask with the desired channel pattern. The photoresist is developed, and the photoresist and metal in the feature area is removed during the development process. Wet etching of glass is mostly done in hydrofluoric acid (HF)-containing solutions. The remaining metal and photoresist are removed from the substrate. Finally, the

etched substrate is then bonded to a second substrate containing drilled reservoir holes, to form a finished microchip.

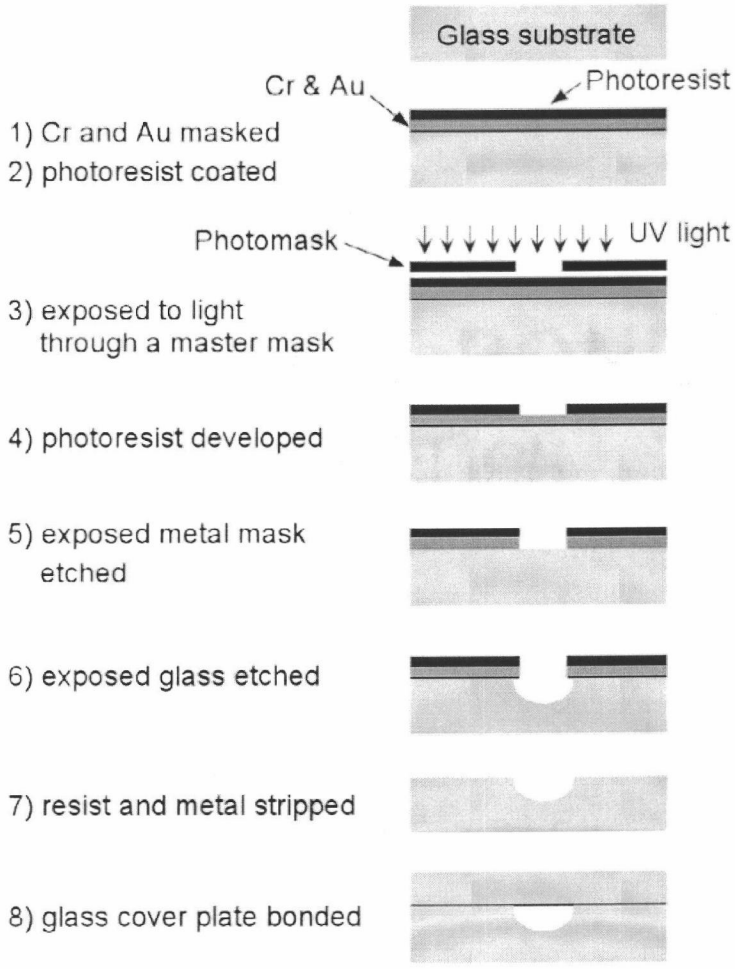

Fig. 4.1. Photolitographic process for fabricating microchip glass devices [19]

While UV absorbance has been the most widely used detection method in conventional CE systems, it is not commonly used for microchips because the short optical path lengths offer limited sensitivity. Therefore, fluorescence detection has been the method of choice for most microchip applications due to its high sensitivity, even though most analyte species do not fluoresce naturally, and thus need to be chemically derivatized for detection.

Here we present, for the first time, the use of microchip capillary electrophoresis and fluorescence detection to separate PAMAM dendrimers of various generations. The goal of this work is to extend the application of glass CE microchips for separations of macromolecules. Glass microfluidic chips were fabricated by Micralyne, Inc. (Micralyne Inc., Edmonton, AB, Canada) and laser-induced fluorescence was employed for the detection of fluorescently labeled dendrimers.

4.2 Experimental

4.2.1 Chemicals

Starburst PAMAM dendrimers with an EDA core, of different generations (5-20% solution in methanol), were purchased from Aldrich (Milwaukee, WI, USA). 5-carboxytetramethylrhodamine, succinimidyl ester (TAMRA) was from Molecular Probes Inc. (Eugene, OR, USA). Dimethyl sulfoxide (DMSO) was purchased from EMD Chemicals, Inc. (Gibbstown, NJ, USA). Sodium phosphate (dibasic) and sodium phosphate (monobasic) were from Sigma (St. Louis, MO,

USA). Reagent grade sodium hydroxide and hydrochloric acid were from J.T. Baker (Phillipsburg, NJ, USA).

4.2.2 Microchip CE instrument

All microchip electrophoresis experiments were performed on a Micralyne Microfluidic Tool Kit (μTK) instrument (Micralyne Inc., Edmonton, AB, Canada) as depicted in figure 4.2 b). The system consists of high voltage (HV) power supplies coupled with a green laser-induced fluorescence (LIF) detection system containing a 532 nm frequency-doubled Nd-YAG laser (4 mW), a dichroic beam splitter, a 550 nm long-pass filter, a 568.2 nm bandpass filter and a PMT detector. The μTK instrument was controlled by LabView software (National Instruments, Austin, TX, USA).

Glass microchips used for the experiments were supplied by Micralyne (Micralyne Inc., Edmonton, AB, Canada). The design of the microchip is shown in figure 4.2 a. The microchip is made from two pieces of low fluorescence Schott Borofloat^{TM} glass, featuring a twin-T injection design of 16 x 95 x 2.2 mm. The length of the twin-T intersection in this design is 100 μm. The bottom piece contains the etched pattern and the top piece contains the reservoir holes. Each microchip consists of a short and long channel, each of 9.64 and 90.28 mm, respectively. The short (injection) channel serves to load the sample from the sample well, whereas the long (separation) channel serves to separate the sample within the intersection of the two channels electrophoretically by changing the applied electrical potential. The channels are D-shaped in cross-section of 20 μm

depth and 50 μm width at the top. The channel wells have a diameter of 2 mm and depth of 1.1 mm. The wells are labeled sample reservoir (SR), sample water (SW), buffer reservoir (BR), and buffer waste (BW).

TAMRA (5-carbocytetramethylrhodamine, succinimidyl ester) (fig. 4.3) was chosen as the fluorophore in accordance with the green laser-induced fluorescence (LIF) detection used for the experiments, which excites at a wavelength of 532 nm and detects at 570 nm. The detection distance was set at 35 mm from the intersection of the injection and separation channels.

(a)

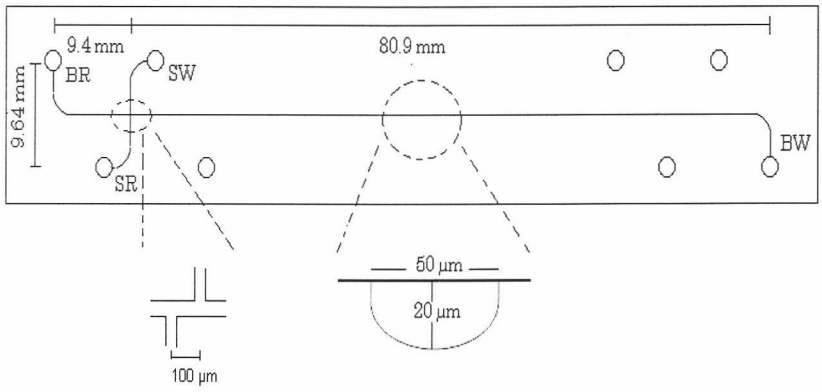

(b)

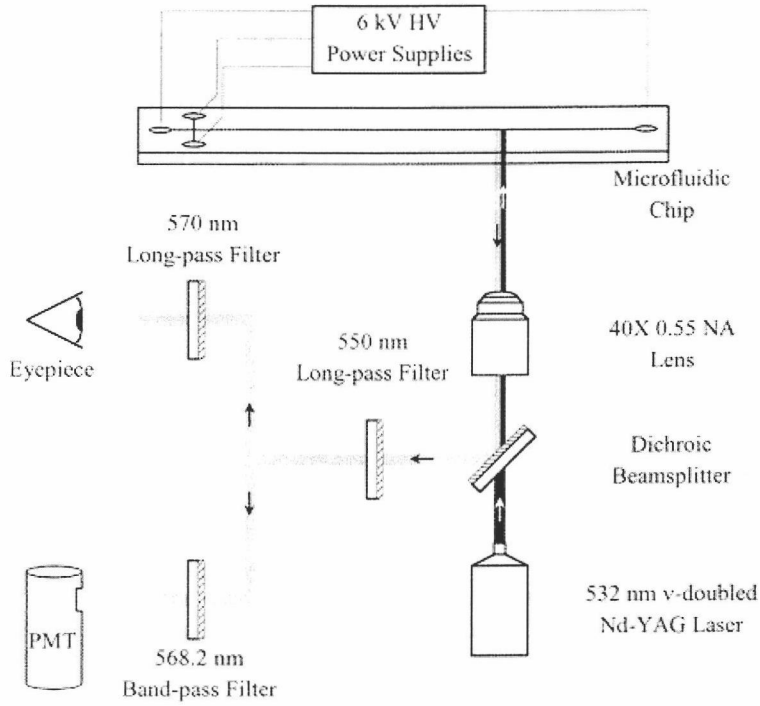

Fig. 4.2 (a) Design of the microfluidic glass chip used for electrophoretic experiments (Micralyne Inc.), BR: buffer reservoir, BW: buffer waste, SR: sample reservoir, SW: sample waste; (b) A block diagram of the Micralyne Microfluidic Tool Kit instrument (μTK) consists of high-voltage power supplies coupled with a green laser-induced fluorescence (LIF) detection system [20].

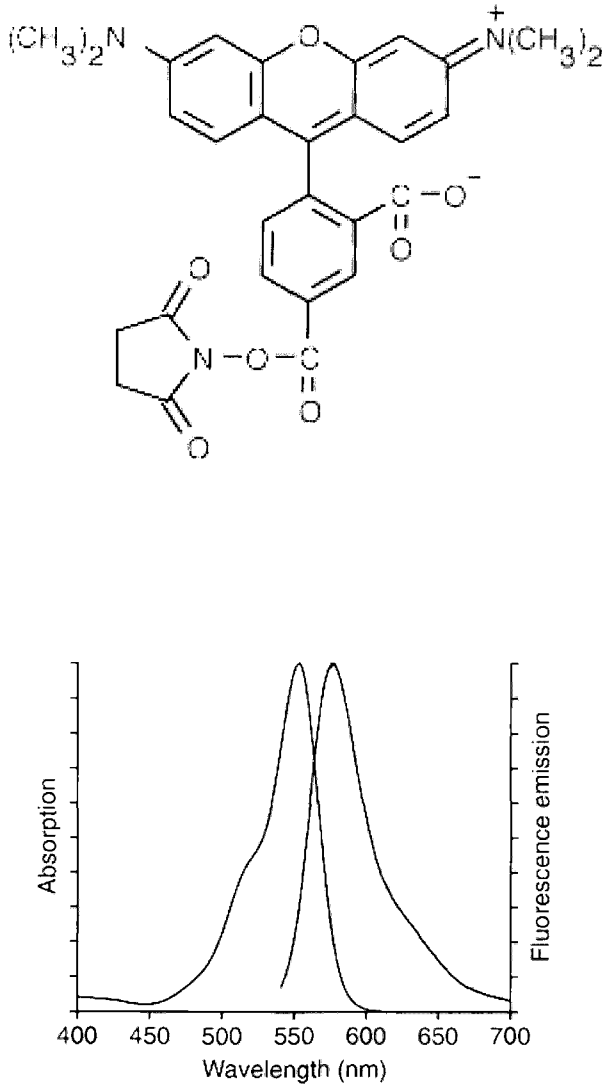

Fig. 4.3 Structure of 5-carboxytetramethylrhodamine, succinimidyl ester (5-TAMRA, SE) (top), Absorption and fluorescence emission spectra of 5-TAMRA, SE in pH 7 buffer (bottom) [21]

4.2.3 Dendrimer labeling

The dendrimer was derivatized with 5-TAMRA-SE using a procedure developed in our lab. First, dendrimer solutions of different generations (2-10 mg/mL) were prepared individually in pH 8.3 sodium bicarbonate 0.1 M after removal of methanol by evaporation. TAMRA (10 mg/mL) was dissolved in DMSO immediately prior to use. Appropriate amounts of TAMRA solutions were then added to dendrimer solutions, and the reactions were carried out at room temperature in the dark with continuous stirring overnight. The solutions of TAMRA-labeled dendrimers were then diluted to give a final concentration of 2 μM in 50mM phosphate buffer pH 2.7 solution and were kept at 4°C until use.

4.2.4 Microchip CE experiment

The microchip was silanized and conditioned in a manner similar to that used for the fused-silica capillary experiments (see chapter 3.2.2.1). Before each injection, the chip was conditioned by washing sequentially with 1M H_3PO_4, millipore H_2O, 1M NaOH, H_2O, and running buffer. Chip conditioning was done by applying a vacuum to one reservoir and filling the other three reservoirs with the appropriate solution. At the end of each day, the microchip was cleaned with NaOH and H_2O, and was stored in H_2O.

All solutions were loaded manually into the microchip using a micropipette. A 1-mL plastic syringe was used for applying vacuum to one

reservoir. The running buffer was loaded into the buffer reservoir, buffer waste and sample waste (3 μL each). The sample solution was loaded into the sample reservoir (3 μL).

The two-step voltage program used is summarized in table 4.1. The first step forms a sample plug at the channel intersection with voltages applied to the sample reservoir, buffer reservoir, and buffer waste while holding the sample waste at ground. The second step injects the plug down the separation channel toward the detector. During this step, voltages were applied to the buffer reservoir, while the buffer waste was held at ground.

	Injection (kV)	Separation (kV)
BR	1.10	6.00
BW	2.00	Ground
SR	1.50	5.20
SW	ground	5.20
Duration (sec)	20	300

Table 4.1. Two-step voltage program used for TAMRA-labeled dendrimer separations

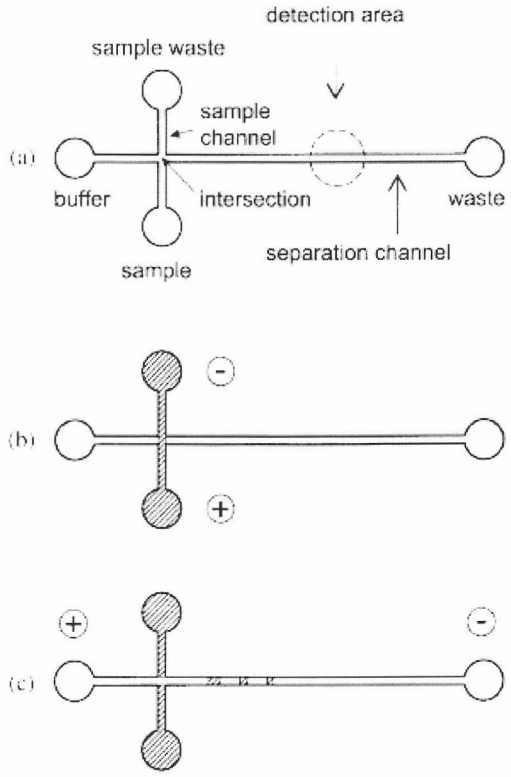

Figure 4.4. Schematic diagram of CE microchip principle, (a) plug (pinched) injection step to introduce narrow, well-defined plug of sample into channels, (b) separation step to inject the plug down the separation channel toward the detector.

4.3 Results and discussion

A schematic diagram of microchip CE experiment is represented in fig 4.4. After the buffer solutions are introduced into SW, BR, and BW, a small and well-defined amount of sample can be injected into the channel by using plug (or pinched) injection. At first, the sample is loaded onto the sample reservoir, and potential (typically 1500 V) is applied between sample and sample waste reservoirs. At the same time, small potentials are also applied at the buffer and buffer waste reservoirs to prevent sample leakage into the separation channel, which is caused by diffusion and convective flow and may happen if the channels are left floating. In this way, the sample solution fills the sampling channels through the intersection and a well-defined sample plug can be obtained (fig. 4.4 a).

During the separation step, the sample mixture to be separated is transported through the separation channel. A potential difference (typically 6000 V) is applied between BR and BW reservoirs and some voltage was applied to SR and SW. In this way, the sample solution in the intersection area is pulled into the separation channel, while leakage of sample and "pull-back" of any remaining sample in the intersection are prevented. The plug is separated into its components depending on their charge and size (fig. 4.4 b). The twin-T design, where the two side channels are offset by a certain distance, is mainly used for this injection mode in order to increase the volume to be injected and thus, increase overall analytical sensitivity. Optical detection using the laser-induced fluorescence technique was carried out at a distance of about 35mm from the intersection area.

As mentioned before, although fluorescence detection offers high sensitivity, it has a limitation in terms of the necessity of most analyte species to be chemically derivatized prior to analysis. This is not a simple task, as some analytes lack the appropriate the functional groups for functionalization.

Full-generation PAMAM dendrimers with their terminal amino groups can be conjugated to succinimidyl esters since they can form a stable amide bond between the dye and dendrimer. The conjugation reaction can be seen in fig 4.5. 5-TAMRA-SE (amine-reactive fluorescence dye) reacts with the non-protonated amine terminus of full-generation PAMAM dendrimers. The terminal amine of a PAMAM dendrimer has a pKa of between 9 and10. Thus, the conjugation must take place in an alkaline solution in order to maintain the amine group in the non-protonated form. 0.1 M sodium bicarbonate buffer, pH 8.3, was used for the experiment since it does not contain primary amines, and thus would not compete for conjugation with the amine-reactive dye.

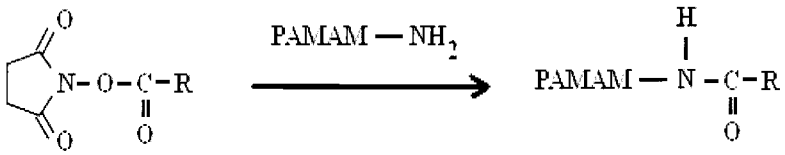

Fig. 4.5. Conjugation reaction of PAMAM full-generation dendrimers and 5-TAMRA-SE (R is tetramethylrhodamine)

Separation conditions were optimized for the electrophoretic separation of TAMRA-labeled dendrimers in glass microfluidic channels. The method used for the analysis was transferred from the on-column CE method into the glass microchips. The same pH, composition, and ionic strength of the running buffer were used for the separation. The results are shown in fig. 4.6. The assignment of peaks was based on single runs of each dendrimer. Generation 0 and 2 PAMAM dendrimers were successfully separated and detected in 50 mM phosphate buffer, pH 2.7, with a retention time of about 60 seconds for G2. The electric field employed was 660 V/cm. The detection distance was set at 35 mm from the intersection of the injection and separation channels.

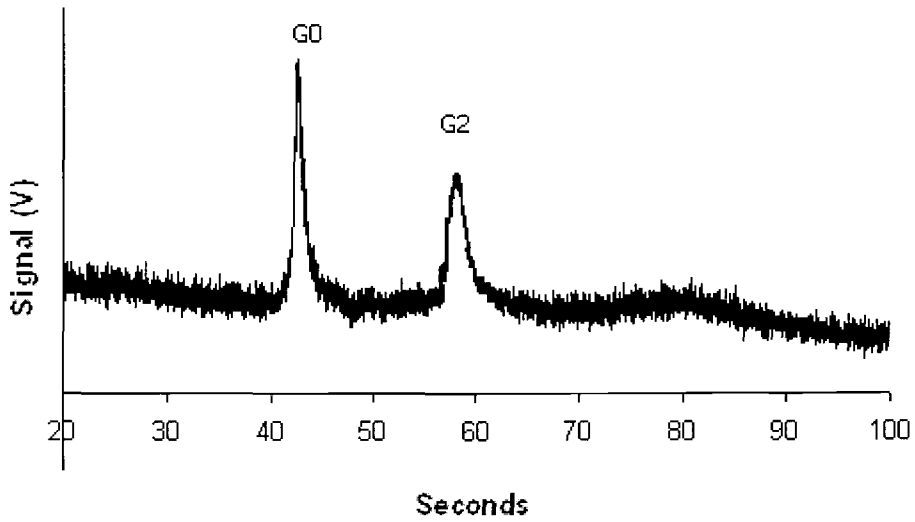

Fig. 4.6. Electropherogram of TAMRA-labeled PAMAM generation 0 and 2 dendrimer in 50 mM phosphate buffer pH 2.7 using glass microchip.

The separation efficiencies were calculated for each peak in the electropherogram. Plate numbers, N, were calculated using the peak width at half height, $w_{1/2}$ [22]:

$$N = 5.54\,(t_r / w_{1/2})^2 \qquad (4.1)$$

The peaks were resolved in approximately 60 s with separation efficiencies of 1.03×10^5 and 3.03×10^4 plates/m for G0 and G2, respectively. The sample volume injected into the separation channel was ~100 pL; thus the detected amount corresponds to 2×10^{-10} μmol at a concentration of 2 μM.

4.4 Conclusions

The findings indicate the feasibility of using microchip capillary electrophoresis and fluorescence detection to separate PAMAM dendrimers of various generations. The method was successfully transferred from the on-column CE method into channels of glass microfluidic devices for rapid dendrimer analysis. Microchip analytical systems have several potential advantages for the determination of dendrimers. These include fast analysis times, small sample volume requirements, and the ability to integrate several steps of analysis in one chip.

References

[1] Manz, A.; Graber, N.; Widmer, H.M. *Sens. Actuator, B Chem.*, B1, 1-6, **1990**, 244

[2] Dolnik, V.; Liu, S. *J. Sep. Sci.* **2005**, *28*, 1994–2009

[3] D.R. Reyes, D. Iossifidis, P.A. Auroux, A. Manz, *Anal. Chem.* **2002**, *74*, 2623.

[4] P.A. Auroux, D. Iossifidis, D.R. Reyes, A. Manz, *Anal. Chem.* **2002,** *74*, 2637.

[5] J. Wang, G. Chen, M.P. Chatrathi, A. Fujishima, D.A. Tryk, D. Shin, *Anal. Chem.* **2003**, *75*, 935.

[6] M. Pumera, *Talanta* **2005**, *66*, 1048.

[7] G.J.M. Bruin, *Electrophoresis* **2000**, *21*, 3931.

[8] V. Dolnik, S. Liu, S. Jovanovich, *Electrophoresis* **2000**, *21*, 41.

[9] A.J. Gawron, R.S. Martin, S.M. Lunte, Eur. *J. Pharm. Sci.* **2001**, *14*, 1.

[10] T. Vilkner, D. Janasek, A. Manz, *Anal. Chem.* **2004**, *76,* 3373.

[11] Manz, A.; Fettinger, J. C.; Verpoorte, E.; Ludi, H.; Widmer, H. M.; Harrison, D. J. *Trends Anal. Chem.* **1991**, *10*, 144.

[12] Jacobson, S. C.; Hergenroder, R.; Koutny, L. B.; Warmack, R. J.; Ramsey, J. M. *Anal. Chem.* **1994**, *66*, 1107.

[13] J.C. McDonald, J.R. Anderson, D.T. Chiu, H. Wu, O.J.A. Schueller, G.M. Whitesides, *Electrophoresis*, **2000,** *21*, 27.

[14] C. Wu, R. Wu, J. Huang, Y. Lin, H. Chang, *Anal. Chem.* **2003**, *75,* 947.

[15] J. Wang, M. Pumera, G.E. Collins, A. Mulchandani, *Anal. Chem.***2002**, *74*, 6121.

[16] M. Pumera, J. Wang, F. Opekar, I. Jelinek, J. Feldman, H. Lowe, S. Hardt, *Anal. Chem.* **2002**, *74*, 1968.

[17] J.D. Harrison, A. Manz, Z.H. Fan, H. Ludi, H.M. Widmer, *Anal. Chem.* **1992**, *64*, 1926.

[18] S.C. Jacobson, R. Hergenroder, L.B. Koutny, J.M. Ramsey, *Anal. Chem.* **1994**, *66*, 1114.

[19] Kikutani, Y.; Tokeshi, M.; Sato, K..; Kitamori, T. *Pure Appl. Chem.*, **2002**, *74*, 2299–2309.

[20] Crabtree, H.J.; Cheong, E.; Tilroe, D.A.; Backhouse, C. *Anal. Chem.* **2001**, *73*, 4079-4086.

[21] Haugland, R. (Ed.), *Handbook of Fluorescent Probes, 9th ed.,* Molecular probes, Eugene, OR USA **2003**

[22]Meyers, R.A. (Ed.). *Encyclopedia of Analytical Chemistry*, Ramtech, Chichester, UK **2000**

CHAPTER 5

CONCLUSIONS

As mentioned before, our group, as part of an interdisciplinary team, is working on developing a nanoextraction technology for coupling to high yield polyamidoamine (PAMAM) dendrimer syntheses. Impurities occasionally arise during synthesis of these dendrimers, and therefore, to achieve higher purity products, chromatographic separations of dendrimers are an important part of a high-yield microreactor system. This thesis explored approaches toward this objective, focusing in two areas: first, development of materials and devices that will enable separations of dendrimers in confines of capillary and chromatographic columns, and second, evaluation of the feasibility of transferring the previously developed separation techniques to the channels of microfluidic devices. This chapter summarizes the main findings of this study and draws out major conclusions and future work.

PAMAM dendrimers of various generations were successfully analyzed using capillary zone electrophoresis (CZE), capillary electrochromatography (CEC), and high-performance liquid chromatography (HPLC). Although a complex separation mechanism results, CZE provided fast and efficient separations of various full-generation dendrimers. Generational separations up to the fifth generation were achieved in acidic conditions. Homogeneity and the presence of side products in the synthesized dendrimers were also assessed by this method.

As HPLC is widely used in many chemical laboratories, separations of dendrimers by HPLC were also investigated. Findings from this study indicated that HPLC can be used for analysis of these macromolecules. Full-generation separations up to generation 5 were achieved using an RP-HPLC method. Separations of dendrimers with terminal amino and carboxyl groups, that were not possible by CE, were obtained using HPLC.

In order to generate highly selective sorbents that can be used for separations of various generations, particularly for high generation dendrimers, a methacrylate-based monolithic stationary phase was developed. In this study, PAMAM dendrimers were utilized as template molecules for preparing porous monolithic sorbents. The concept of dendrimer-templating is not new for our research group. Previously, dendrimer templates were used to affect the porosity of finished monolithic polymers. A similar approach was used in this work; however, this time dendrimers not only were used as template molecules for controlling pore structures, but also for generating selective sorbents in the form of imprinted polymers with surfaces containing sites that are complementary in chemical functionality to the dendrimer template molecule.

A simple and quick method for the in situ preparation of monolithic columns with dendrimer-templated were prepared for CEC. At first, dendrimer molecules were incorporated into a solution of functionalized monomers, cross linkers, solvent, and initiator. Thermal polymerization, followed by the removal of the solvent and dendrimers, produced a continuous rod of polymer with uniform porosity and controlled surface chemistry. This approach has delivered sorbents

with higher selectivity. Separations of dendrimers of various generations were achieved using these sorbents.

The first step toward the development of a nanoextraction technology for high yield dendrimer syntheses was to evaluate the feasibility of transferring the separation techniques developed on-column into a microchip format. The suitability of using a voltage-driven separation technique (CE) in a microchip format for dendrimer application was investigated. Glass microfluidic chips and laser-induced fluorescence detection were employed for this purpose. Although fluorescence detection offers high sensitivity, dendrimers do not fluoresce naturally, and thus need to be chemically derivatized for detection. The results, however, have indicated that microchip capillary electrophoresis and fluorescence detection can be used to separate PAMAM dendrimers of various generations. These findings have proven the applicability of microchip analytical systems for the determination of dendrimers. Advantages of this system include rapid analysis, small sample volume requirements, and the ability to integrate several steps of analyses all in one chip, from sampling, sample processing, and separation to detection.

In conclusion, this work has opened a new chapter in the development of materials and devices for the separation of PAMAM dendrimers. Lately, the development of polymers, such as poly(dimethylsiloxane) (PDMS) and poly(methyl methacrylate) (PMMA), as microchip substrates are emerging for micro technology due to their low cost and ease of fabrication. In future work, separations of dendrimers using these materials will be explored using the methods

developed in this study. To achieve higher selectivity sorbents, dendrimer-templated monoliths can also be prepared by casting them in situ in the microchips. These monoliths can then be used as sorbents for dendrimer separations.